Naval Research Reviews

Office of Naval Research
Three / 1992
Vol XLIV

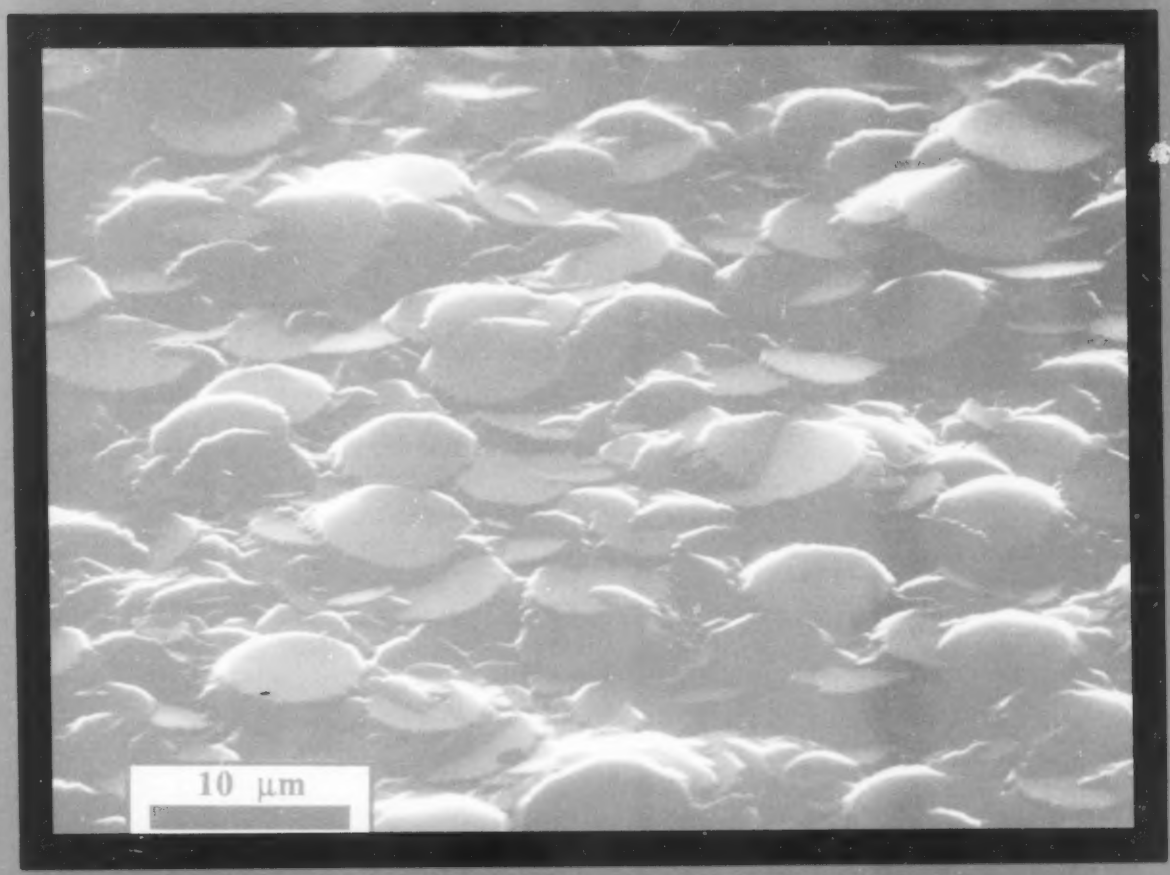

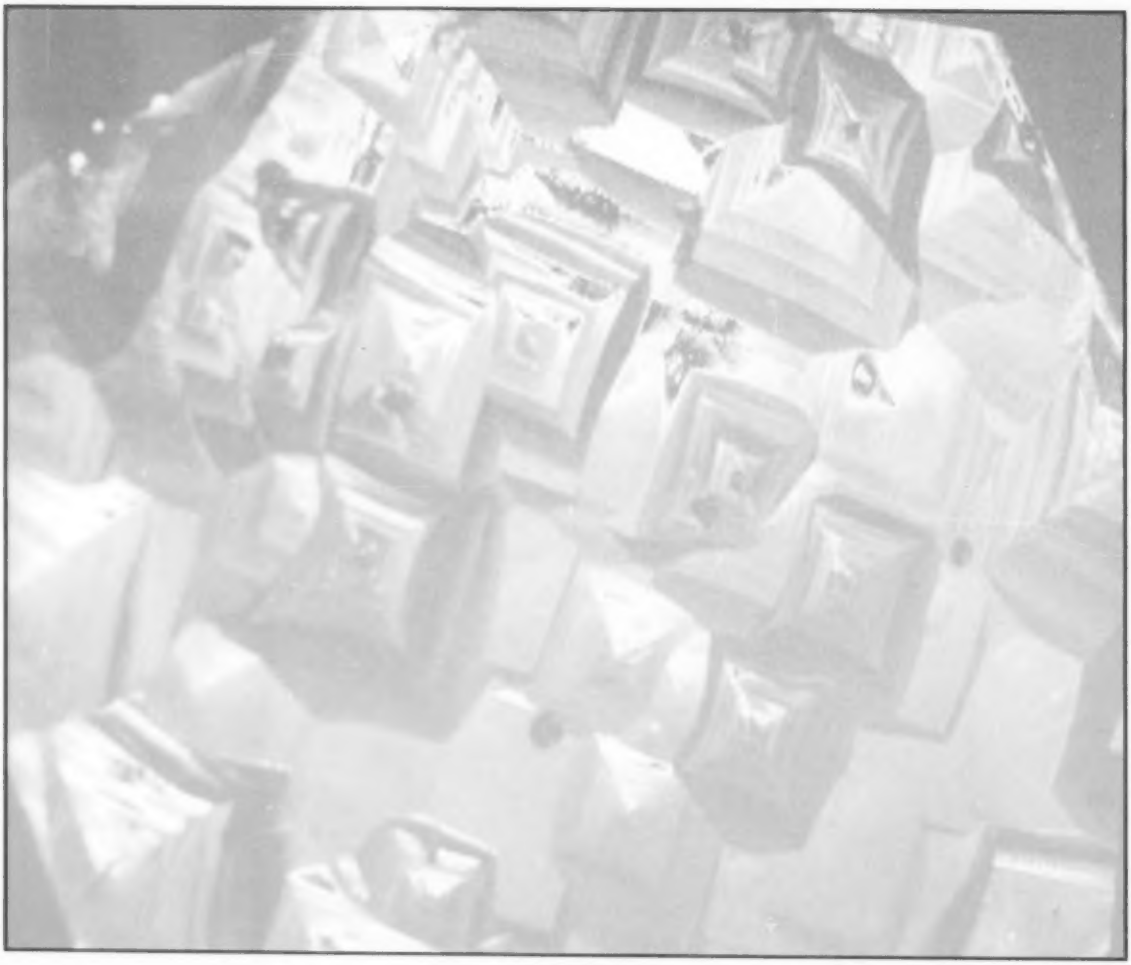

Scanning laser microscope image of homo-epitaxial diamond grown on a diamond seed crystal using an oxy-gen-acetylene torch in atmosphere. This research is part of an ongoing study funded by the Office of Naval Research to better understand how diamonds grow. Single crystal diamond films may form the basis of high speed, high temperature, radiation hard micro-electronics.

Naval Research Reviews

Office of Naval Research
Three / 1992
Vol XLIV

Articles

2
Introduction
Lawrence Kabacoff

3
Diamond: The Ultimate Durable Infrared Window Material
Daniel C. Harris

17
Diamond: Its Impact On Electronics
Max N. Yoder

23
Diamond Chemical Vapor Deposition
F. G. Celii
J. E. Butler

Departments

22
Profiles in Science

45
Research Notes

CHIEF OF NAVAL RESEARCH
RADM William C. Miller, USN

DIRECTOR
Dr. Fred Saalfeld

CHIEF WRITER/EDITOR
William J. Lescure

SCIENTIFIC EDITORS
Dr. Robert J. Nowak
Dr. J. Dale Bultman

MANAGING EDITOR
Norma Gerbozy

ART DIRECTION
Typography and Design
Desktop Printer, Arnold, MD

About the Cover

"Pennies" on the surface of a diamond film grown in a microwave plasma reactor at the Naval Air Warfare Center at China Lake. Note the 10 micrometer marker bar. This unusual microstructure is observed midway between a region of square crystal faces and a much less crystalline region. The rounded faces arise from square faces whose corners are nicked off. ONR-sponsored research at China Lake supports an effort to develop diamond as a durable infrared-transmitting window material for Navy weapons systems. The photo is by C.E. Johnson (see article by Harris in this issue on page 2.)

Naval Research Reviews publishes articles about research conducted by the laboratories and contractors of the Office of Naval Research and describes important naval experimental activities. Manuscripts submitted for publication, correspondence concerning prospective articles, and changes of address, should be directed to Code OPARI, Office of Naval Research, Arlington, VA 22217-5000. Requests for subscriptions should be directed to the Superintendent of Documents, U.S. Government Printing Office, Washington, DC 20403. *Naval Research Reviews* is published from appropriated funds by authority of the Office of Naval Research in accordance with Navy Publications and Printing Regulations. NAVSO P-35.

Introduction

Lawrence Kabacoff,

Materials Division, Office of Naval Research

Diamond has been a subject of fascination since its discovery in India more than 3000 years ago. The science of diamond dates from the discovery in 1797 that it is a crystalline form of carbon. Through the years, scientific interest in this hardest of all materials has grown due to its astonishing variety of extreme properties. For example, diamond is a very wide band gap semiconductor (5.5 eV). In an undoped state, it has the largest electrical resistivity and breakdown voltage known. When doped (for example, with boron), it exhibits very high electron and hole mobility (superior to Si, GaAs, and InP). Diamond has the highest known room temperature thermal conductivity (2.5 times that of copper) and a coefficient of thermal expansion less than invar. It is the stiffest known material, is highly transparent to infrared radiation, and even has an extremely low coefficient of friction. These, and other properties have made diamond the most studied material in existence.

For years, scientists and engineers could only be tantalized by these properties because diamonds were only obtainable as gem stones in small sizes and at very great expense. The first breakthrough came in the 1950's with the development and commercialization, by General Electric, of a high temperature, high pressure (HTHP) process for economically producing artifact diamond. The HTHP process is practical only for the production of small diamond particles suitable for such applications as polishing and cutting.

The second breakthrough came with the discovery by William Eversol that diamond could be deposited on a substrate by chemical vapor deposition (CVD). Initially, deposition rates were depressingly low, of the order of 0.01 microns/hr. Throughout the late 1950's and 1960's, Boris Deryagin and coworkers in the Soviet Union investigated ways of greatly increasing these deposition rates. These results were not widely believed because he would not reveal the experimental conditions used. Starting in 1974, The National Institute for Research in Inorganic Materials (NIRIM) in Japan made enormous strides in the practical synthesis of diamond films and coatings. This strong Japanese research and development effort continues to the present.

Some research on low pressure synthesis (LPS) of diamond was being pursued in the United States, by John Angus at Case Western Reserve University and others; however, widespread interest in this country really began when Dr. Rustum Roy, returning from visits to NIRIM and Soviet laboratories, alerted the Office of Naval Research to Japanese and Soviet work in this area. ONR responded by providing funding to launch a vigorous research effort. Following the successful fabrication of diamond films by Dr. Roy, the Innovative Science and Technology Office within the Strategic Defence Initiative Organization, and later the Defense Advanced Research Projects Agency joined ONR in supporting research programs in LPS artifact diamond. This has lead to important advances, both in our understanding of diamond synthesis, and in the exploitation of diamond films, coatings, and structures for both military and civilian applications.

In this issue of *Naval Research Reviews*, three aspects of LPS artifact diamond research of prime importance to the Navy are described. In the first article, Dan Harris of the Naval Surface Warfare Center at China Lake, California, describes efforts to exploit diamond technology in the development of a new generation of infrared domes and optics. Next, Max Yoder of ONR, reviews the important opportunities available in the field of doped diamond semiconductors for high temperature, radiation resistant integrated circuits. Finally, James Butler of the Naval Research Laboratory discusses how diamond grows during the LPS process and the factors that influence growth rate and film quality. In each of these important areas of technology, The Navy has assumed a leadership role, both through research and development programs carried out at Navy Laboratories and in promoting and funding fundamental research by industry and academia. As a result of these efforts, the commercialization and exploitation of this most extraordinary material is rapidly becoming a reality.

Diamond: The Ultimate Durable Infrared Window Material

Daniel C. Harris
Naval Air Warfare Center, Weapons Division, China Lake, California

The Problem

All objects with temperatures between room temperature and several thousand degrees emit electromagnetic radiation, mainly in the infrared region of the spectrum. Numerous military systems use infrared sensors for guidance, tracking or surveillance because the object being observed is a source of infrared light. For example, the Sidewinder missile in Figure 1 homes in on radiation from the hot exhaust of an aircraft engine. The infrared-transparent dome at the front of the missile protects the delicate infrared sensor from the harsh flight environment.

A critical problem for infrared systems is that *infrared-transparent materials suffer from insufficient resistance to rain and sand erosion and thermal shock.*[1] Figure 2 shows missile domes eroded by collisions with water drops or sand particles in the air during captive carry flight beneath the wing of an airplane. Thermal shock may occur immediately after launch when the front tip of the dome of a rapidly accelerating missile becomes several hundred degrees hotter than parts of the dome just a few centimeters aft. Catastrophic failure of the dome in Figure 2 occurred when the hot tip of the brittle dome expanded much more than the cooler surrounding parts of the dome. While thermal shock failure is limited to high speed missiles in free flight, rain erosion is a problem at aircraft speeds and sand erosion is a problem even for stationary objects on a battlefield.

Diamond Looks Like the Best Solution

Diamond is the most durable candidate for windows and domes among infrared-transmitting materials. Table I compares physical properties of diamond[2] to those of zinc sulfide and sapphire. Zinc sulfide is the only widely used missile dome material for the 8-14 μm wavelength "long wave" atmospheric transmission window (even though zinc sulfide only transmits well from 8 to 10 μm). Sapphire is the most durable material available for the 3-5 μm wavelength "midwave" atmospheric transmission window. Infrared sensors that operate in the atmosphere must use either or both of these bands, because the atmosphere does not transmit radiation outside these bands.[3]

Diamond is a crystalline form of carbon in which each atom is surrounded by four other carbon atoms at the corners of a regular tetrahedron. The crystal contains the highest number density of atoms (1.76×10^{23} atoms/cm^3) of any material. Diamond is the hardest known material, and is therefore most resistant to abrasion by particles. Diamond is extremely strong and stiff, which gives it exceptional resistance to water drop impact damage. The thermal conductivity of diamond is greater than that of any material (including metals) at room temperature, and its thermal expansion is very low. The combination of thermal and mechanical properties allow diamond to withstand more than 100 times as great a heat flux as other dome materials without thermal shock failure.

Table 1.

Comparison of Properties of Diamond, Zinc Sulfide and Sapphire.

	Gem Quality Diamond	Zinc Sulfide	Sapphire
Infrared atmospheric transmission window (μm)	8-14 (bulk) 3-5 (thin coating)	8-10.5	3 - 5
Hardness (kg/mm^2)	9000	230	1600
Strength (MPa)	3000	97	900
Young's modulus (stiffness) (GPa)	1050	75	350
Thermal expansion (x $10^6, K^{-1}$)	1.5	7	8
Thermal conductivity (W/m-K)	2000	17	14
Absorption coefficient (cm^{-1})	0.04 (@10.6 m)	0.08 (@9.3 m)	0.04 (@4.0 m)
Dielectric Constant (35 GHz)	5.61	8.35	9.39 (E ⊥ c)† 11.58(E ∥ c)†
Loss Tangent (35 GHz)	0.0006	0.0024	0.00005 (E ⊥ c)† 0.00006 (E ∥ c)†

†E ⊥ c and E ∥ c refer to the electric field perpendicular and parallel to the optical axis of the crystal.

How Diamond is Made

Industrial diamond abrasive grit has been manufactured for more than 30 years by high-pressure, high-temperature processes that produce powders. A technological breakthrough occurred in the 1980's when it was shown first in the Soviet Union and then in Japan that continuous thin films of diamond could be grown by a gas phase process below atmospheric pressure and at temperatures near 900°C.[4] This made it possible to contemplate using synthetic diamond for optical elements, cutting edges on tools and for heat spreading in electronic circuits, among other applications.

Figure 3 shows two common types of reactors for growing diamond by chemical vapor deposition. The microwave unit at the left is fed with a mixture containing approximately 1% (by volume) methane in hydrogen, perhaps with additions of oxygen and argon. The H_2 and CH_4 molecules are dissociated by microwave energy to create a plasma ball at the center of the reactor. Carbon from the methane forms diamond on suitable substrates such as silicon, copper and molybdenum. Alternatively, many other means of dissociating the molecules may be employed to grow diamond under the right conditions. For example, a direct current torch[5] uses an electric arc to create a plasma jet that is directed onto the surface of a substrate that is cooled to 900°C. Other types of reactors use a hot metal filament or an acetylene welder's torch to activate the gas mixture. Industrial reactors deposit diamond over areas greater than 100 cm^2. From early work with micrometer thick depositions, diamond growth has been scaled up to produce millimeter thicknesses.

Figure 1.

"Heat-seeking" Sidewinder missile. The infrared seeker used to home in on exhaust from a jet engine is located immediately behind the hemispheric infrared-transparent magnesium fluoride dome at the front of the missile.

Figure 2.

Common forms of damage to infrared missile domes: (A) pitting produced by sand in the Persian Gulf; (b) thermal shock failure in T-Range test at China Lake that simulates the heating associated with rapid acceleration; and (c) damage from raindrop impacts during captive carry of the missile under an aircraft wing.

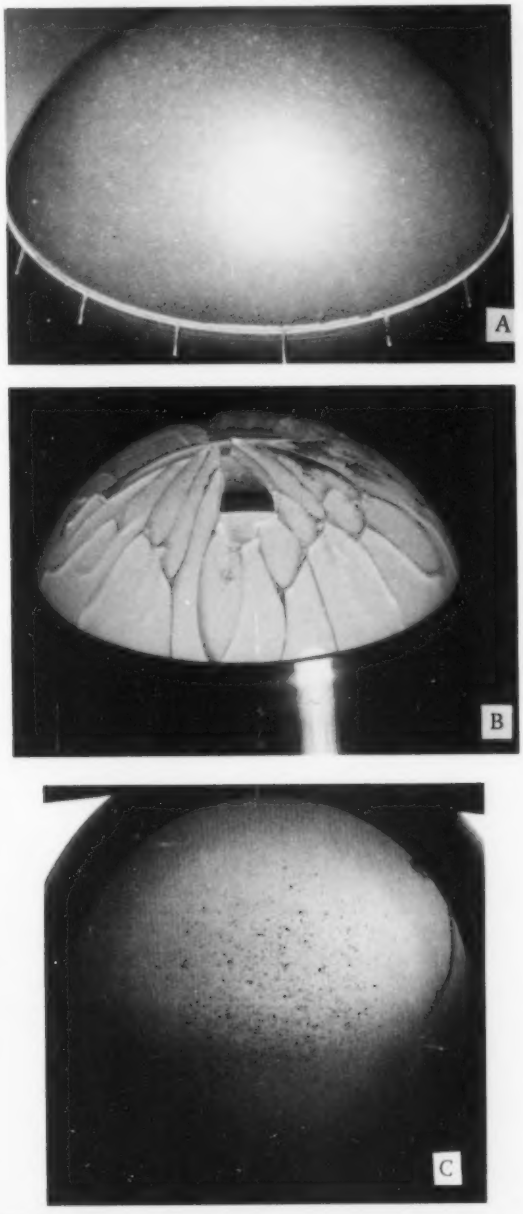

Controlling Morphology and Nucleation

The methods described above usually produce polycrystalline material that consists of randomly oriented microscopic crystals of diamond, as in Figure 4. By adjusting conditions, coarser or finer grain sizes can be grown. The thicker the film, the greater the grain size generally becomes, with grains up to several hundred micrometers observed in diamond whose thickness is near 1 mm. It is also possible to produce selectively oriented crystals, as in Figure 5.[6] In our research scale microwave reactor, square (100) crystal faces predominate in growths with 2% methane in hydrogen and triangular (111) faces are found when 1% oxygen is added to the feedstock. If a particular face predominates, it means that growth occurs preferentially on the other faces around the one that is observed.

Nucleation is a critical determinant of diamond growth morphology. Figure 6A shows densely nucleated, fine grain diamond grown on a silicon substrate that had been abraded for 10 min with a paste containing <0.25 μm diameter diamond particles. The paste was rinsed off thoroughly prior to diamond deposition. This is the most common substrate pretreatment for silicon. Figure 6B shows the result of growth under the same conditions, but without diamond abrasion pretreatment. Only a few nuclei form and they grow into relatively immense particles. Nucleation density and crystal morphology are affected by varying the nucleation method. Figure 6C shows diamond grown on a 0.25 μm thick layer of a refractory nitride that had been sputtered onto silicon. The nitride layer, which was not abraded with diamond powder, nucleates an intermediate density of diamond particles.

An interesting case of nucleation on a noncooperative surface is shown in Figure 7. Diamond does not ordinarily

Figure 3.

Two ways to grow diamond by chemical vapor deposition using a microwave plasma (left) or direct current torch (right).

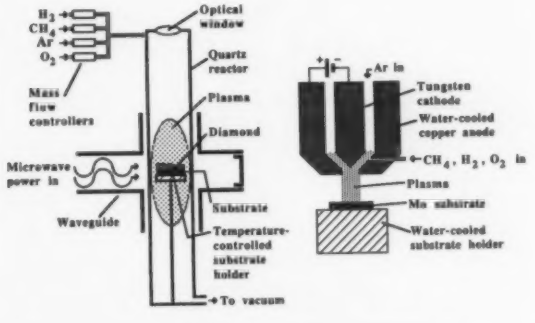

grow on a fused silica surface, even with diamond abrasion. When thin films of certain metals are sputtered onto part of the silica surface, diamond grows on the surface that was *not* covered with metal.

Why do we care about controlling nucleation density and morphology? Different applications of diamond ought to benefit from different microstructures. For example, large grain size gives a greater thermal conductivity,[7] and is therefore preferred for heat spreading in electronic circuits. Large grain diamond probably has less of the nondiamond grain boundary phase found in small grain material, so large grain diamond is probably preferred for enhanced infrared transmission. Mechanical strength is generally related to microstructure, but this phenomenon has not yet been studied for diamond. Internal stress in diamond films varies over several orders of magnitude[8] and is undoubtedly a function of microstructure. Since the difficulty of polishing diamond is a function of crystal face and orientation,[1] it is expected that selective growth of diamond may be a means to reduce the expense of polishing surfaces.

Diamond and Its Carbon Impurities Both Come From Methyl Radical

Although most diamond growers use methane as a readily available source of carbon, diamond can be grown by chemical vapor deposition using almost any volatile carbon compound. Methyl radical, CH_3, is believed to be the gas phase species that accounts for most of the growth of diamond and for much

Figure 4.

Typical microstructure of diamond showing randomly oriented crystallites.

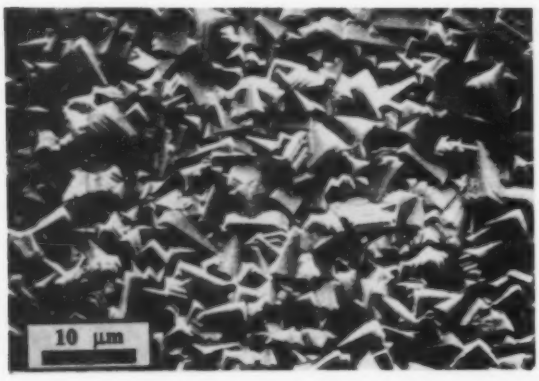

Figure 5.

Oriented growth of polycrystalline diamond in microwave reactor. Square faces (A) predominate in the absence of oxygen, while triangular faces (B) are observed when 1% oxygen is added. Both types of faces are seen in the individual diamond crystallite (C).

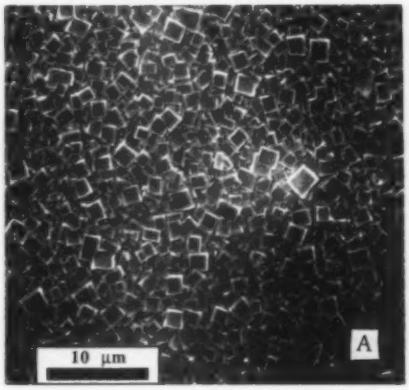

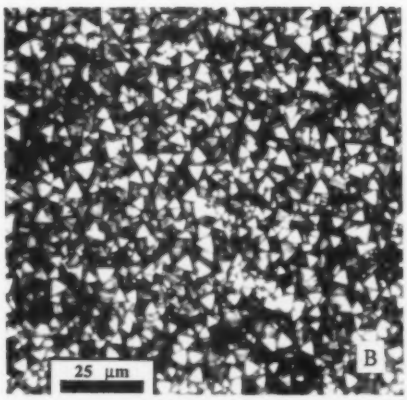

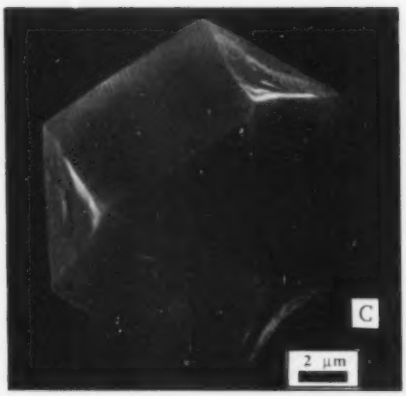

Figure 6.

(A) Densely nucleated, fine grain diamond grown on silicon that had been abraded with diamond and rinsed clean. (B) Growth under the same conditions as (A), but without the diamond abrasion step. Large particles on the surface are diamond. The grain structure of the bare substrate is evident because of etching by the hydrogen plasma during diamond growth. (C) Intermediate nucleation density of diamond on a 0.25 μm thick layer of a refractory nitride deposited on the surface of silicon prior to diamond growth. The nitride layer was not abraded with diamond particles. All growths were for 12 h in the same microwave reactor under the same conditions.

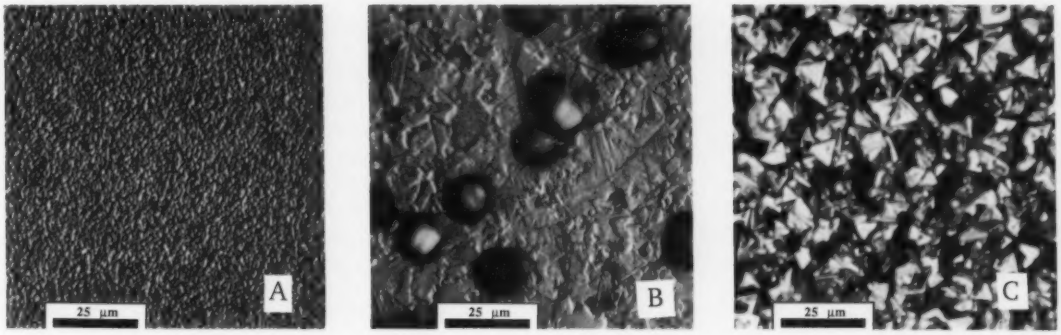

of the codeposition of nondiamond carbon impurities in hydrogen plasma reactors.

The argument for the role of methyl radical in diamond growth begins with experimental[9] and theoretical[10] evidence that methane (CH_4) and acetylene (C_2H_2) are the dominant hydrocarbon species in the gas phase of a hot filament reactor in which either CH_4 or C_2H_2 are used as feedstock in approximately 1% mixture with 99% H_2. The calculated concentration of methyl radical is approximately one tenth that of methane. Other species such as C_2H_4, C_2H_6, C_2H_5, C_2H_3, C_2H, C_3H_6, C_3H_2, C_3H_3, C_3H_4, C_3H_5, etc, are observed or calculated to be orders of magnitude less abundant. Even if their reaction rates were diffusion controlled, none of these minor species is present in great enough concentration to account for the observed rate of diamond deposition. The only species present in high enough concentration to account for the observed growth rate of diamond are CH_4, CH_3 and C_2H_2. While CH_3 and C_2H_2 are reactive molecules that could add to the surface of diamond, CH_4 is not reactive and is not further considered as a candidate. However, CH_4 is the immediate precursor to CH_3 by reactions such as $CH_4 + H = CH_3 + H_2$, where the hydrogen atom is provided by dissociation of hydrogen molecules. Strong kinetic evidence for methyl radical as the precursor to diamond comes from studies in which the growth rate of diamond was proportional to the calculated concentration of CH_3 in the gas phase,[11] but had no consistent correlation with the C_2H_2 concentration.[12]

Convincing evidence for the dominant role of CH_3 over C_2H_2 in diamond growth comes from studies with ^{13}C isotopically labeled reactants.[13-17] Figure 8 compares the Raman spectrum of diamond grown from $^{12}CH_4$ to that of diamond grown from a mixture of ^{13}C-enriched CH_4 plus $^{12}C_2H_2$. The

Figure 7.

Diamond film spelling "NWC" (for the now disestablished Naval Weapons Center) grown on a fused silica disk . The entire surface except where the letters appear was covered with a thin layer of a sputtered metal. When the disk was placed in a microwave plasma reactor, diamond grew on the surface that was not covered by metal. In the absence of the metal, no growth of diamond occurs on fused silica. The fused silica was not abraded with diamond powder prior to growth.

Figure 8.

Raman spectra of diamond films grown in microwave plasma reactor. Material in the upper trace was grown from CH_4 with a natural abundance (99%) of ^{12}C. Material in the lower trace came from a mixture of ^{13}C-enriched CH_4 plus $^{12}C_2H_2$. Dots are experimental points and solid lines were obtained using two gaussian peaks to fit each data set. A Raman spectrum is obtained by passing laser light through a sample and observing scattered light with frequencies that differ from that of the laser. Differences between the incident and scattered radiation correspond to quanta of vibrational energy that are absorbed by the sample.

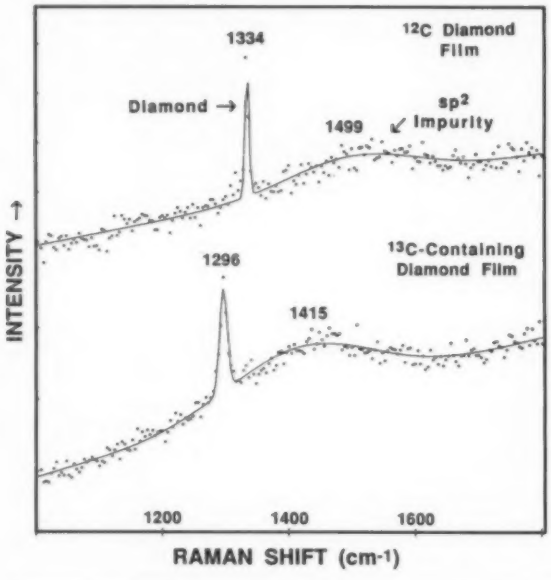

sharp peak at 1334 cm^{-1} in the upper spectrum arises from vibrations of the crystal lattice of ^{12}C-diamond. The broad peak near 1499 cm^{-1} is from graphite-like carbon impurities commonly designated "sp^2." High quality diamond films contain no peak at 1499 cm^{-1}. Carbon-rich growth conditions were intentionally chosen for the experiments in Figure 8 to enhance the sp^2 carbon for study.

Substitution of ^{13}C for ^{12}C in diamond shifts the vibrational band in the Raman spectrum by approximately 50 cm^{-1}, down to 1282 cm^{-1}. In diamond containing some ^{13}C and some ^{12}C, the position of the vibrational band lies between the two limits and can be used to determine how much ^{13}C is present.

If diamond is grown from a mixture of $^{13}CH_4$ and $^{12}C_2H_2$, the ^{13}C content of the diamond indicates how much is derived from CH_3 (which comes from CH_4 in the plasma) and how much comes from C_2H_2. A complication in this experiment is that there is some interconversion of carbon between CH_4 and C_2H_2 (giving $^{12}CH_4$ and $^{13}C_2H_2$) in the plasma during the deposition. For example, in one experiment in which 1.0% $^{13}CH_4$, 0.5% $^{12}C_2H_2$, 0.05% O_2 and 98.45% H_2 was passed through our microwave reactor, the exit gas contained CH_4 with 79% ^{13}C and 21% ^{12}C and C_2H_2 with 31% ^{13}C and 69% ^{12}C. The diamond deposited by this mixture contained 73% ^{13}C, which is considerably closer to the isotopic content of CH_4 than C_2H_2. Considering the relative amounts of CH_4 and C_2H_2 in the reactor, the conclusion of this experiment is that CH_3 (derived from CH_4) is approximately 12 times more efficient than C_2H_2 in producing diamond.

Figure 8 shows that not only does the Raman signal for diamond shift upon ^{13}C incorporation, but so does the sp^2 impurity signal. Therefore a mixture of $^{13}CH_4$ and $^{12}C_2H_2$ could also be used to identify the gas phase precursor to the sp^2 impurity. Figure 9 shows that the shift of the sp^2 peak is correlated much better with the isotopic composition of CH_4 than of C_2H_2.[17] It is concluded that methyl radical, CH_3, is the dominant precursor to carbon in the diamond and in the sp^2 impurity. If we want to increase the growth rate of diamond relative to that of the sp^2 impurity, it cannot be done by enhancing the chemistry leading to methyl radical formation.

Figure 9.

Raman shift of sp^2 impurity in diamond vs. ^{13}C concentration in the gas phase. Open circles are a calibration series of specimens grown from known mixtures of $^{12}CH_4$ and $^{13}CH_4$. Because the sp^2 signal in Figure 8 is broad and weak, its peak position is difficult to measure accurately. Therefore each circle in the calibration curve is an average of several measurements from different samples. Filled triangles show the sp^2 Raman peak position plotted as a function of ^{13}C content of CH_4 when films are grown from mixtures of $^{13}CH_4$ plus $^{12}C_2H_2$. Open squares show the same sp^2 Raman peak positions plotted against ^{13}C content of C_2H_2. Although there is a great deal of noise in the data, the correlation of sp^2 shift with CH_4 ^{13}C content is better than that with C_2H_2 ^{13}C content.

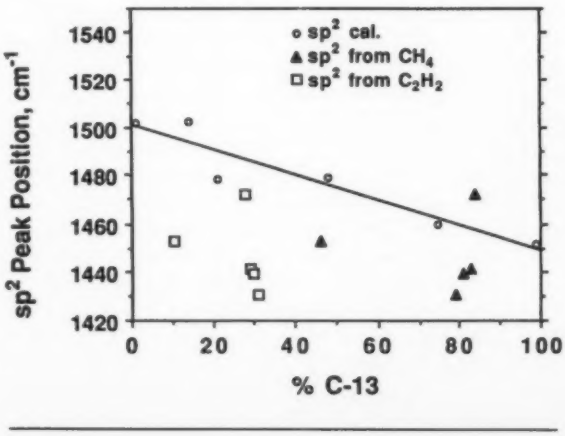

Oxygen is Diamond's Friend and Enemy

Small additions of oxygen to a microwave reactor increase the rate of diamond deposition (Figure 10) and decrease the quantity of sp^2 impurity (Figure 11). The effect on growth rate can be explained with the mechanism in Figure 12, which is adapted from the combustion literature.[18] This sequence of reactions is in qualitative accord with our observations of diamond growth in microwave plasma and direct current torch reactors.[6,17,19,20] Small additions of O_2 increase the diamond growth rate because oxygen atoms and OH radicals participate in the conversion of CH_4 to CH_3 at the upper left of Figure 12. That is, addition of oxygen to the plasma increases the concentration of methyl radical, which is the immediate precursor to diamond.

Figure 10 showed that the diamond growth rate goes through a maximum and then further addition of oxygen decreases the growth rate.[6] Too much oxygen (a) removes methyl radical from the gas phase (by initial oxidation to C_2H_2O and eventually to CO and CO_2) and (b) etches away diamond that has already been deposited. Some etching is desirable because the sp^2 impurity is etched more rapidly than diamond. This explains why the quality of the diamond deposit increases with increasing oxygen addition in Figure 11, even though the net growth rate is decreasing. A small amount of oxygen is helpful for producing higher quality diamond in a microwave reactor.

Figure 10.

Diamond growth rate in a microwave reactor in which the feedstock contains a 2:97 mole ratio of CH_4:H_2 with various additions of O_2 (expressed as a mole percent).[6]

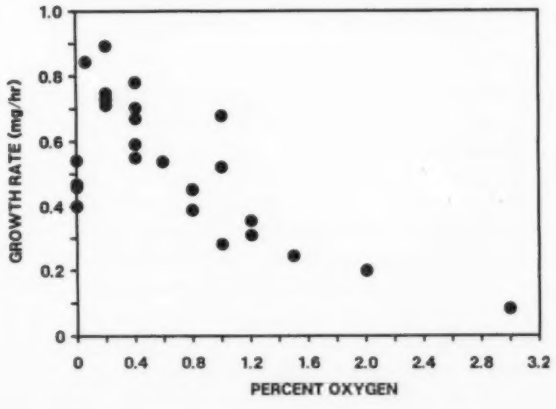

Diamond burns in the presence of O_2 at elevated temperature. Figure 13 shows that combustion of diamond becomes significant at temperatures above approximately 700° C in the air.[21] In the absence of oxygen, but at sufficiently high temperature (~1500° C), diamond spontaneously transforms into graphite,[22,23] which is the thermodynamically stable form of carbon at ambient pressure.

Two Ways to Use Diamond for Infrared Windows and Domes

Once we know how to grow high quality diamond, how can it be used as an infrared window or dome? Figure 14 shows the infrared transmission spectrum of gem quality natural diamond (dashed line) and infrared optical quality artificial diamond. The two are nearly identical in the 8-14 μm long wave atmospheric window. Since diamond reflects 29% of infrared light at normal incidence, and since we observe 71%

Figure 11.

Effect of O_2 addition on sp^2 impurity content of diamond films.[6]

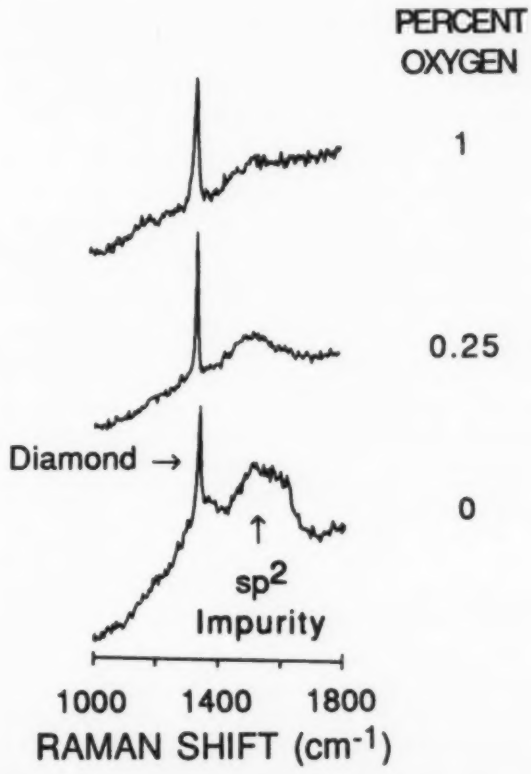

Figure 12.

The mechanism of interconversion of C_1 and C_2 species proposed for combustion[18] explains many observations of plasma chemistry in diamond deposition.

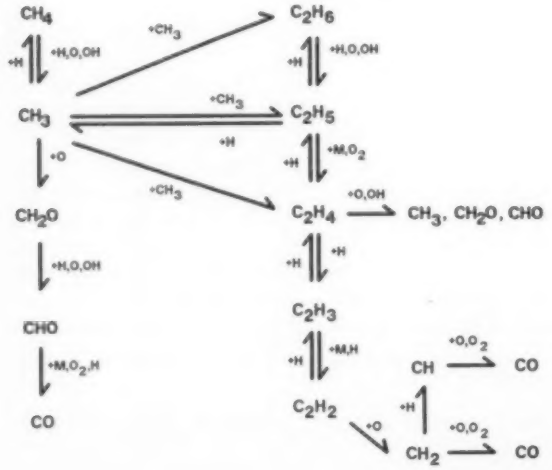

transmission in the long wave window, there is essentially zero absorption by the diamond. In contrast to the long wave behavior, weak absorption bands in the 3-5 μm midwave region reduce the transmission of natural and synthetic diamond below 71%. In addition, synthetic diamond scatters some light at wavelengths below 4 μm, which further reduces its transmission below that of natural diamond in Figure 14.

Figure 15 illustrates the use of diamond as a bulk material or thin protective coating. Bulk diamond windows and domes up to several millimeters thick will be transparent enough for the long wave atmospheric window, but not the midwave window. Protective coatings of diamond up to several tens of micrometers in thickness will be sufficiently transparent for the midwave region. The excellent microwave transmission properties of natural diamond in Table I suggest that bulk diamond and thin films of diamond will be also be useful apertures for dual mode sensors employing both infrared and microwave radiation.

Bulk Diamond

In order to realize the full potential of diamond, the properties of synthetic material must be similar to those of natural diamond. We saw in Figure 14 that the infrared transmission is similar, at least in the long wave window. Mechanical properties of chemical vapor deposited diamond such as modulus[24] and hardness[25] are also similar to those of natural

Figure 13.

Graph shows thermogravimetric experiment in which the mass of a diamond film is measured while it is heated in the air at a rate of 20C/min.[21] Photograph shows partially oxidized diamond surface that may be compared to a representative unoxidized surface in Figure 4.

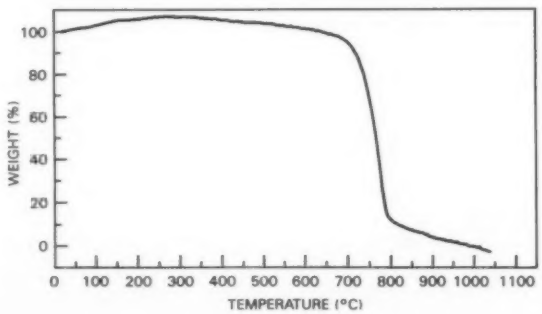

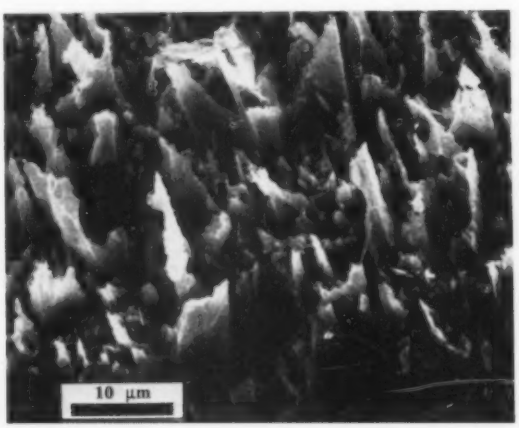

diamond, while the tensile strength is reported to be approximately one fourth as great as that of natural material.[26] Since the strength of a brittle material is a strong function of its fabrication method and the quality of its surface finish, there is no reason to believe that the strength of synthetic diamond is limited to one fourth that of natural diamond. The extraordinary thermal conductivity of natural diamond, which is greater than that of copper near 25°C, is essentially matched by that of synthetic diamond.[1,7,27] It is clear from properties already attained that synthetic diamond will be two orders of magnitude more resistant to thermal shock than any other infrared window material.

What about the durability of diamond with respect to water and particle impact? Figure 16 shows a characteristic

Figure 14.

Infrared transmission spectrum of gem quality natural diamond (dashed line) and artificial diamond (solid line) of the same thickness (0.33 mm) grown at Norton Company. A transparent material has a transmission of 1, while an opaque material has a transmission of 0. Boxes show the midwave (3-5 m) and long wave (8-14 μm) atmospheric transmission windows in which the atmosphere does not absorb infrared radiation.

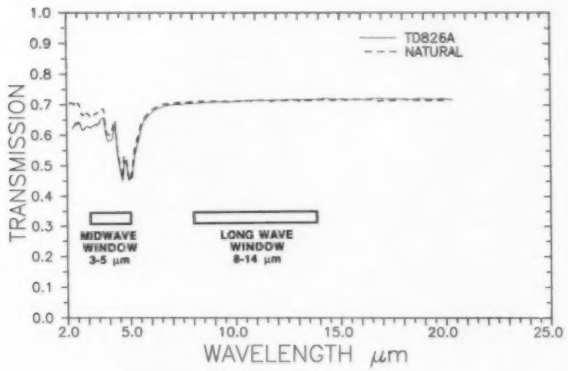

ring fracture produced by a waterdrop impact on a thin film of diamond. A key property of a window or dome material is the threshold velocity below which it is not damaged by waterdrop impact. The threshold measured for natural diamond is 600 m/s for multiple impacts at the same site by 2 mm diameter drops.[28] This threshold is about 10% greater than that of sapphire, which is the most durable available infrared window material. In a study of sand erosion at an impact speed of 26 m/s, the rate of loss of mass by natural diamond was 2×10^4 times lower than the rate of mass loss by silicon nitride (at an impact speed of 47 m/s) and 3×10^6 times lower than the rate of mass loss by alumina (at an impact speed of 34 m/s).[29] In sand impact studies of synthetic diamond, transgranular fracture was observed,[26] which means that fracture lines went right through individual crystallites of the diamond, rather than around them. This implies that grain boundaries of synthetic diamond are strong and that the erosion resistance of synthetic diamond should be similar to that of natural diamond.

Since diamond is more resistant to abrasion than any other material, it is also the most difficult material to polish to an optical finish. Other very hard materials are polished with diamond abrasive. Polishing bulk diamond with diamond grit produces usable infrared optical surfaces (Figure 17) but this process is inefficient. Surface treatment with lasers, ion beams, oxidation and dissolution in iron have been reported, but none has been perfected for optical polishing of diamond and more work is needed in this area.

Figure 15.

Two ways to use diamond: as a bulk material (left) or thin protective coating (right). The 7 cm diameter dome at left was made at Norton Company to demonstrate the capability to grow the required size and shape, but the diamond is not optical quality. The zinc selenide infrared window at the right was coated with an 8 μm thick diamond film at Westinghouse Science and Technology Center using the optical brazing technique in Figure 18.

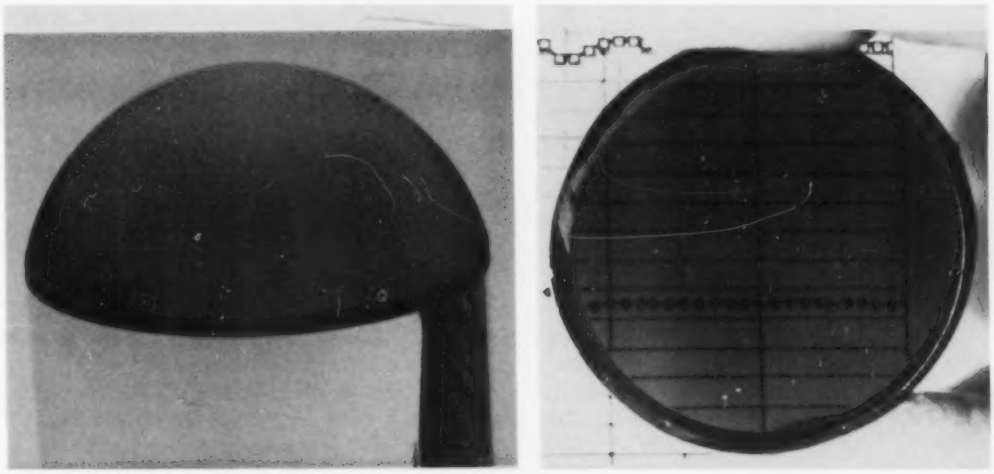

Figure 16.

Impact site of a 20 μm thick diamond film struck by a 2 mm diamond waterdrop.

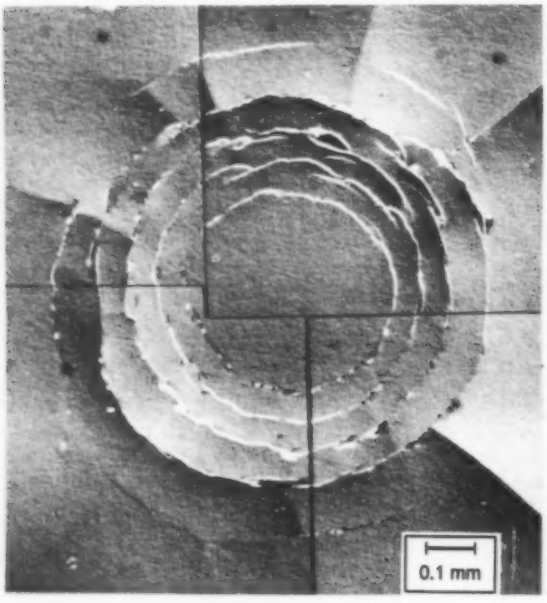

Figure 17.

(A) Unpolished rough surface of diamond that is > 1mm thick and finished surface produced by polishing with a diamond abrasive grit. These samples were produced at Raytheon Co. by microwave plasma dsposition and cut into circular shapes by laser maching. (B) Surface features of polished diamond (with a root-mean-square roughness of 7 nm) grown with a direct current torch at Texas Instruments.

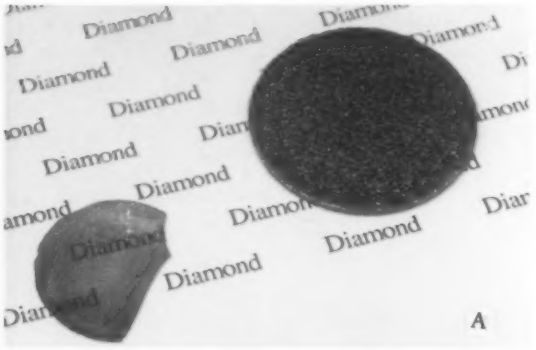

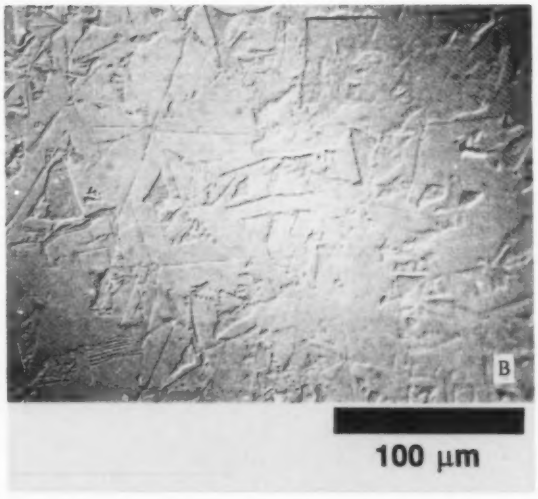

Diamond-Coated Infrared Windows

Attempts to deposit thin, protective coatings of diamond directly on the surface of infrared windows have failed, either because the harsh environment of the reactor attacked the window or because of the mismatch in thermal expansion between diamond and most other materials. Alternative schemes for separately fabricating the diamond and "gluing" it onto the window have been more successful.

Figure 18 outlines an ingenious scheme dubbed "optical brazing" at Westinghouse.[30,31] In this process diamond is first grown on a silicon substrate. The growth surface is rough, as in Figure 5, and the substrate side is nearly as smooth as the optically polished silicon substrate. A sandwich is then made with a low melting, infrared-transparent glass bonding layer between the diamond and the zinc selenide or zinc sulfide window. When the sandwich is hot pressed, the glass flows into all of the valleys in the diamond surface and forms a bond between the diamond and the window material. The silicon is then chemically etched away, exposing the smooth surface of diamond. The key feature of optical brazing is that the bonding glass has the same refractive index as diamond, eliminating optical scatter from the rough diamond growth surface (Figure 19).

Another way to attach diamond to an infrared window (Figure 20) is with a polymeric organic "glue" whose refractive index is different from that of diamond.[32] Index matching anti-reflection coatings are used on both surfaces facing the polymer to reduce reflection losses.

Figure 18.

Optical brazing process[30,31] for attachment of diamond to zinc selenide or zinc sulfide infrared windows using an infrared-transparent glass bonding layer whose index of refraction is matched to that of diamond to reduce scatter from the rough diamond surface.

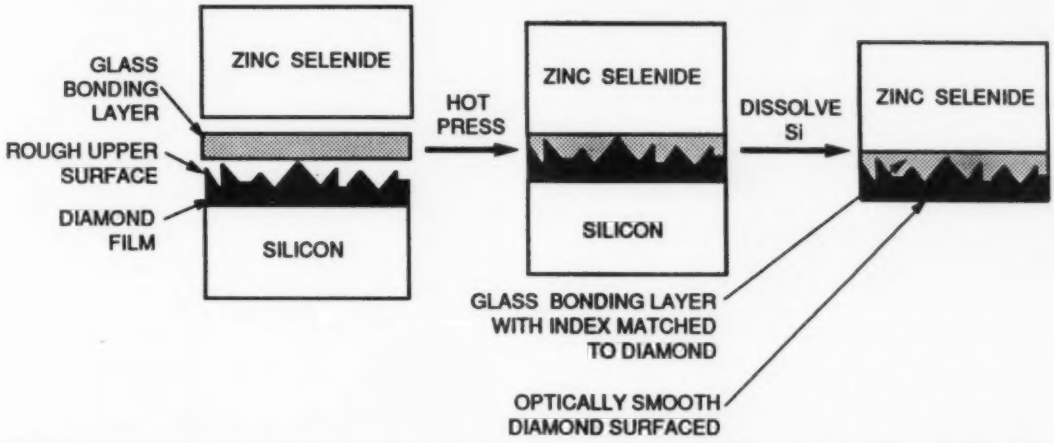

Both optical braze and polymer glue are relatively low temperature materials that are not stable at the ultimate operating temperature of diamond. While these coating technologies should find many uses in systems such as aircraft sensor windows that do not become very hot, the most demanding high temperature applications of diamond require bonding schemes that have yet to be discovered.

Anti-Reflection and Anti-Oxidation Coatings

When light passes between media of different refractive index, some light is reflected at the interface. In a system with many interfaces, reflection losses must be minimized to allow enough light to reach the detector. If the indexes of refraction of two media are n_1 and n_2, a layer with refractive index $\sqrt{n_1 n_2}$ and a thickness that is one fourth of the wavelength of light will reduce reflection from the interface to near zero at the chosen wavelength. This is the purpose of the two internal-anti-reflection layers in Figure 20.

A diamond/air interface reflects 29% of infrared light at normal incidence. Since the index of refraction of diamond is 2.38 and that of air is 1.00, an anti-reflection coating with an index of refraction $\sqrt{2.38 \cdot 1.00} = 1.54$ is required. Because diamond burns in air above 700°C (Figure 13), an ideal anti-reflection coating would also protect diamond from attack by oxygen. Several proprietary anti-reflection/anti-oxidation coatings have been demonstrated, but more work is required to extend the upper operating temperatures. Figure 21 shows the performance of a coating that protects diamond up to 800°C in the air.

An obvious flaw in overcoating diamond with another material is that the outer layer is less durable than diamond. For this reason, the patterned, all-diamond "moth eye" structure[33] in Figure 22 is under investigation. This layer reduces reflection by smoothly grading the effective refractive index from that of air to that of diamond. A disadvantage of an all-diamond moth eye is that no oxidation protection is provided.

Figure 19.

Effect of optical brazing on infrared transmission.

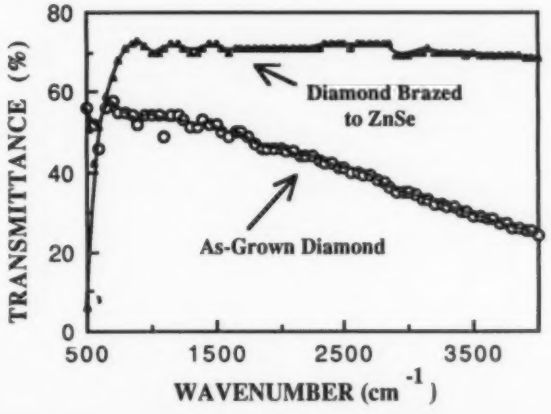

Figure 20.

Polymer glue can be used to bind a thin, protective coat of diamond to a germanium window. Anti-reflection layers are required on both sides of the glue. The outermost anti-reflection layer on top of the diamond is a moth's eye structure, as shown in Figure 22.

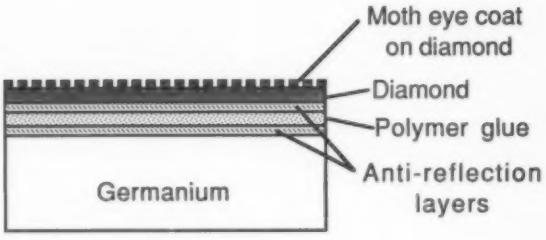

Figure 21.

Anti-reflection coating: Heavy line shows transmission spectrum of a zinc sulfide window. Fine line shows the same window with an optically brazed diamond coating and a proprietary anti-reflection/anti-oxidation overcoat optimized for transmission in the 8-10 μm wavelength region.

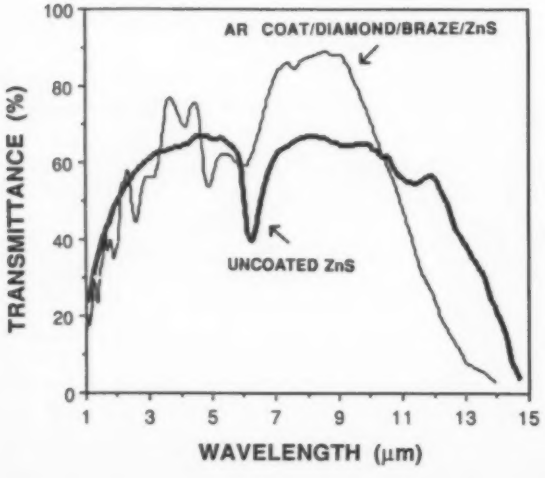

Figure 22.

"Moth eye" diamond anti-reflection structure on the surface of diamond, all grown by chemical vapor deposition at Rockwell Science Center.

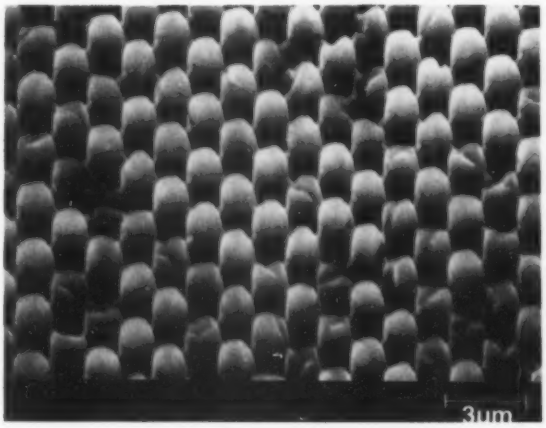

Prospects

Diamond has progressed from a research curiosity to a developmental optical material. Near term goals that are essential for affordability include reproducible fabrication of millimeter thick optical quality material, increased deposition rate and more efficient polishing procedures. While hurdles remain to be conquered, diamond is here to stay as an infrared optical window for the most demanding applications.

Acknowledgements

Research at China Lake featured in this article was carried out by Curtis E. Johnson, Linda F. Johnson, Karl Klemm, Mark B. Moran and Wayne A. Weimer. The overall program was initiated by Robert W. Schwartz. This work was supported by the Office of Naval Technology, the Office of Naval Research, and the Independent Research program at China Lake.

Biography

Dan Harris works in the Optical and Electronic Materials Branch at the Naval Air Warfare Center at China Lake, where he manages materials research and development programs. He holds a Bachelor's degree in chemistry from Massachusetts

Institute of Technology and a Ph.D. in chemistry from California Institute of Technology. Prior to coming to the Naval Air Warfare Center in 1983, he taught chemistry at the University of California at Davis and Franklin and Marshall College in Lancaster, Pennsylvania. He recently wrote the tutorial textbook *Infrared Window and Dome Materials* published by SPIE Press. He is also author of the leading undergraduate textbook in analytical chemistry, *Quantitative Chemical Analysis*, and co-authored the textbook *Symmetry and Spectroscopy*. On those rare occasions when he is not at his desk, he can be found climbing mountains with his sons or camping with Boy Scouts.

References

1. D. C. Harris, *Infrared Window and Dome Materials*, SPIE Optical Engineering Press, Bellingham, Washington (1992).
2. J. Wilks and E. Wilks, *Properties and Applications of Diamond*, Butterworth Heineman, Oxford (1991).
3. R. H. Hudson, Jr., *Infrared System Engineering*, Wiley, New York (1969).
4. K. E. Spear, "Diamond – Ceramic Coating of the Future," *J. Am. Ceram. Soc.*, **72**, 171-191 (1989).
5. F. M. Cerio and W. A. Weimer, "Construction of an Inexpensive DC Plasma Jet for Diamond Deposition Using Commercially Available Components," *Rev. Sci. Instrum.*, **63**, 2065-2068 (1992).
6. W. A. Weimer, F. M. Cerio and C. E. Johnson, "Examination of the Chemistry Involved in Microwave Plasma Assisted Chemical Vapor Deposition of Diamond," *J. Mater. Res.*, **6**, 2134-2144 (1991).
7. J. E. Graebner, S. Jin, G. W. Kammlott, J. A. Herb and C. F. Gardinier, "Unusually High Thermal Conductivity in Diamond Films," *Appl. Phys. Lett.*, **60**, 1576-1578 (1992); J. E. Graebner, S. Jin, G. W. Kammlott, B. Bacon, L. Seibles and W. Banholzer, "Anisotropic Thermal Conductivity in Chemical Vapor Deposition Diamond," *J. Appl. Phys.*, **71**, 5353-5356 (1992).
8. N. S. Van Damme, D. C. Nagle and S. R. Winzer, "Stress in Thick Diamond Films Deposited on Silicon," *Appl. Phys. Lett.*, **58**, 2919-2920 (1991).
9. F. G. Celii, P. E. Pehrsson, H.-T. Wang and J. E. Butler, "Infrared Detection of Gaseous Species During the Filament-Assisted Growth of Diamond," *Appl. Phys. Lett.*, **52**, 2043-2045 (1988); S. J. Harris, A. M. Weiner and T. A. Perry, "Measurement of Stable Species Present During Filament-Assisted Diamond Growth," *Appl. Phys. Lett.*, **53**, 1605-1607 (1988); C.-H. Wu, M. A. Tamor, T. J. Potter and E. W. Kaiser, "A Study of Gas Chemistry During Hot-Filament Vapor Deposition of Diamond Films Using Methane/Hydrogen and Acetylene/Hydrogen Gas Mixtures," *J. Appl. Phys.*, **68**, 4825-4829 (1990); S. J. Harris and L. R. Martin, "Methyl Versus Acetylene as Diamond Growth Species," *J. Mater. Res.*, **5**, 2313-2319 (1990).
10. D. G. Goodwin and G. G. Gavillet, "Numerical Modeling of the Filament-Assisted Diamond Growth Environment," *J. Appl. Phys.*, **68**, 6393-6400 (1990).
11. S. J. Harris, A. M. Weiner and T. A. Perry, "Filament-Assisted Diamond Growth Kinetics," *J. Appl. Phys.*, **70**, 1385-1391 (1991).
12. S. J. Harris and A. M. Weiner, "Diamond Growth Rate vs. Acetylene Concentrations," *Thin Solid Films*, **212**, 201-205 (1992).
13. C. J. Chu, M. P. D'Evelyn, R. H. Hauge and J. L. Margrave, "Mechanism of Diamond Film Growth by Hot-Filament CVD: Carbon-13 Studies," *J. Mater. Res.*, **5**, 2405-2413 (1990).
14. M. P. D'Evelyn, C. J. Chu, R. H. Hauge and J. L. Margrave, "Mechanism of Diamond Growth by Chemical Vapor Deposition: Carbon-13 Studies," *J. Appl. Phys.*, **71**, 1528-1530 (1992).
15. C. J. Chu, M. P. D'Evelyn, R. H. Hauge and J. L. Margrave, "Mechanism of Diamond Growth by Chemical Vapor Deposition on Diamond (100), (111) and (110) Surfaces: Carbon-13 Studies," *J. Appl. Phys.*, **70**, 1695-1705 (1991).
16. C. E. Johnson, W. A. Weimer and F. M. Cerio, "Efficiency of Methane and Acetylene in Forming Diamond by Microwave Plasma Assisted Chemical Vapor Deposition," *J. Mater. Res.*, **7**, 1427-1431 (1992).
17. C. E. Johnson and W. A. Weimer, "Mass Spectrometry Studies of Diamond Deposition," *Proc. SPIE*, **1759** (1992).
18. J. Warnatz, in *Combustion Chemistry* (W. C. Gardiner, ed.), Springer-Verlag, New York (1984).
19. F. M. Cerio, W. A. Weimer and C. E. Johnson, "Diamond Growth Using Carbon Monoxide as a Carbon Source," *J. Mater. Res.*, **7**, 1195-1203 (1992).
20. W. A. Weimer and C. E. Johnson, "Diamond CVD Growth Chemistry," *Proc. SPIE*, **1759** (1992).
21. C. E. Johnson, M. A. S. Hasting and W. A. Weimer, "Thermogravimetric Analysis of the Oxidation of CVD Diamond Films," *J. Mater. Res.*, **5**, 2320-2325 (1990).
22. T. Evans and P. F. James, "A Study of the Transformation of Diamond to Graphite," *Proc. Roy. Soc. London*, **A277**, 260-269 (1964).
23. G. Davies and T. Evans, "Graphitization of Diamond at Zero Pressure and at a High Pressure," *Proc. Roy. Soc. London*, **A328**, 413-428 (1972).
24. G. F. Cardinale and R. W. Tustison, "Biaxial Modulus Measurement of Chemical Vapor Deposited Polycrystalline Diamond Films," *J. Vac. Sci. Technol. A*, **9**, 2204-2209 (1991).
25. C. J. McHargue, "Mechanical Properties of Diamond and Diamond-Like Films," in *Applications of Diamond Films and Related Materials* (Y. Tzeng, M. Yoshikawa, M.

Murakawa and A. Feldman, eds.), Elsevier, Amsterdam (1991).

26. Z. Feng, Y. Tzeng and J. E. Field, "Solid Particle Impact of CVD Diamond Films," *Thin Solid Films*, **212**, 35-42 (1992).
27. D. T. Morelli, T. M. Hartnett and C. J. Robinson, "Phonon-Defect Scattering in High Thermal Conductivity Diamond Films," *Appl. Phys. Lett.*, **59**, 2112-2114 (1991).
28. C. R. Seward, C. S. J. Pickles, R. Marrah and J. E. Field, "Rain Erosion Data on Window and Dome Materials," *Proc. SPIE*, **1760** (1992).
29. I. P. Hayward and J. E. Field, "The Solid Particle Erosion of Diamond," *J. Hard Mater.*, **1**, 53-64 (1990).
30. W. D. Partlow, R. E. Witkowski and J. P. McHugh, "CVD Diamond Coatings for the Infrared by Optical Brazing," in *Applications of Diamond Films and Related Materials* (Y. Tzeng, M. Yoshikawa, M. Murakawa and A. Feldman, eds.), Elsevier, Amsterdam (1991).
31. R. H. Hopkins, W. E. Kramer, G. B. Brandt, J. S. Schruben, R. A. Hoffman, K. B. Steinbruegge and T. L. Peterson "Fabrication and Evaluation of Erosion-Resistant Multispectral Optical Windows," *J. Appl. Phys.*, **49**, 3133-3139 (1978).
32. A. B. Harker and J. F. DeNatale, "Diamond Gradient Index "Moth-Eye" Antireflection Surfaces for LWIR Windows," *Proc. SPIE*, **1760** (1992).
33. J. F. DeNatale, P. J. Hood, J. F. Flintoff and A. B. Harker, "Fabrication and Characterization of Diamond Moth Eye Antireflective Surfaces on Ge," *J. Appl. Phys.*, **71**, 1388-1393 (1992).

Diamond: Its Impact On Electronics

Max N. Yoder
Office of Naval Research

Uniqueness

Why should diamond have an impact on electronics? Given a matrix of materials and their properties, the values for diamond will almost always represent either a minima or a maxima of the values for all materials for any given property. The efficacy of diamond as a material useful for electronic applications ensues from selected **combinations** of those minima and maxima values. Table 1 provides selected properties of diamond that are relevant to electronics applications.

Negative Electron Affinity

Perhaps the most intriguing property of diamond is the negative electron affinity (NEA) of its {111} crystallographic face. Why the {111} diamond surface alone should exhibit this property is not currently understood. Not only does this surface exhibit NEA, but it is extremely robust in that its cold cathode (electron emitting) properties are not poisoned by exposure to atomic oxygen, atomic hydrogen, air, or water[2]. Since virtually all vacuum tubes in use today are poisoned when cathode ambient pressure rises above 10^{-7} Torr, the robust nature of a diamond cathode could be particularly attractive for use in adverse environments. Diamond cathodes constructed of p-n junctions of single crystalline diamond emit with current densities as high as 10 A/cm^2.[2] Although this emission density is commensurate with many vacuum tube requirements (e.g., CRTs), most semiconductors are capable of current densities exceeding 10^5 A/cm^2 – and diamond should exceed this by a factor of ten. The potential thus exists for significantly increasing the emission density as well. Diamond is an indirect bandgap semiconductor with the energy minima lying along the {111} direction. This may be relevant in the experimental evidence that the electrons are ejected tangential to the {111} surface. The apparent monoenergetic nature of the emitted electrons (e.g., 4.5 eV) may also prove useful in reducing electron beam noise in vacuum tubes. In contrast to the built-in wear-out mechanism (e.g., amperes times hours is a constant) in thermionic cathodes, there appears as yet to be no such limitation on diamond cathodes. Deliberate arcing of diamond cathodes sufficient to destroy adjacent metallization does not destroy the NEA properties of the diamond surface.[2] NEA has also been exhibited on the {111} surfaces of polycrystalline diamond.[3]

Transistors

The high field drift velocity of both electrons and holes in diamond surpasses that in all other materials; its hole mobility is exceeded only by that in germanium. Its electron mobility exceeds that of silicon. By virtue of its exceedingly high dielectric strength combined with its unsurpassed charge car-

Table 1.

Selected Diamond Properties

Property	Value	Units
Dielectric Constant	5.61	
Dielectric Strength	1.0×10^7	V/cm
Dielectric loss	6.0×10^{-4}	Tangent
Refractive index	2.4	
Bandgap	5.45	eV
Hole mobility	1.6×10^3	cm^2/V-sec
Hole velocity	1.0×10^7	cm/sec
Electron mobility	2.2×10^3	cm^2/V-sec
Electron velocity	2.7×10^7	cm/sec
Resistivity	1.0×10^{13}	ohm-cm
Thermal Conduct.	20.0	W/cm-°K
Thermal Exp. Coef.	1.1×10^{-6}	°K
Work Function	-4.5	eV *
Lattice Constant	3.57	Angstroms

* on {111} surface only[1]

rier velocity, its figure of merit for use as a high power, high performance amplifier can be calculated by the method of Johnson[4] to be 8200 times that of silicon. For use in densely packed integrated circuits, the low dielectric constant and the unsurpassed thermal conductivity are also exploited. Using the method of Keyes[5] it can be shown that the performance of diamond in this application exceeds that of silicon by a factor of 32. Since the bandgap of diamond is so large, there are virtually no thermally excited charge carriers at temperatures up to 500° C. Charge carriers from impurity dopants are, however, more heavily scattered at high temperatures. Even then, the performance of a 500° C diamond FET has been calculated to exceed that of a GaAs FET operating at 20° C.[6,6] Conventional inversion mode FETs use a back-doped channel to reduce off-state leakage current. In diamond, this should not be necessary as the intrinsic leakage of diamond – even at elevated temperatures – is virtually non-existent. The large bandwidth also renders diamond immune to exciton generation by IR and visible light thus eliminating noise from such sources.

Variations of conventional transistor structures are also of interest for high power diamond amplifiers. These structures consist of intrinsic (undoped, insulating) diamond with degenerately doped "source" and "drain" contacts placed at an interruption of a transmission line on the diamond surface. The excitation of the gap region is by either energetic electron beam (EBIC) or by UV laser. Thyristors of diamond are also conceivable, but like any bipolar device fabricated of diamond, the forward-bias voltage drop of 5.5 volts can be excessive for certain applications. In very high voltage switches, however, this drop is less than that of the series-connected silicon device equivalent.

Photodectors

Conventional photodetectors use reverse-biased p-n junctions. The p-n junctions are required to reduce leakage current such that dynamic range may be maximized. By virtue of the large bandgap in diamond, there is no measurable leakage (dark) current at temperatures below 500° C. Therefore, a diamond photodetector is a simple MIM structure resembling a parallel plate capacitor. The metal contacts are non-injecting for both holes and electrons; charge carriers can only be extracted from the diamond into the metallization in the manner of Goodman.[7] The absence of the p-n junction has one additional advantage: the electric field is uniform; thus holes and electrons experience the same field and there is much less pulse dispersion. The similarity of electron and hole mobilities in diamond also lowers signal dispersion. Being an indirect gap material, optical absorption between 5.45 eV and 7.0 eV (direct gap minima) is weak, but absorption is strong above 7 eV.

"Solar cells" of diamond diodes have also been demonstrated.[2] Diamond diodes have generated output power effi-

ciency as high as 40% of the illuminating 100 MeV electron beam energy. These devices could be constructed as batteries to replace lower efficiency thermionic sources for spacecraft power supplies.

A combination detector of alpha particles and gamma rays is envisioned with intrinsic insulating diamond. For the alpha particle detection, a simple interdigitated ohmic metallization pattern on a diamond surface would suffice while the gamma rays would require ohmic metallization of the back surface of the diamond. Such a device, of course, is immune from background noise generated by IR or visible light. As such, it could serve as a low cost radon detector.

Resistors and Capacitors

By virtue of its unsurpassed thermal conductivity, resistors made by implanting carbon ions into diamond exhibit equally unsurpassed dissipation per unit area. Unless degenerately implanted, however, a temperature dependant thermistor results. Resistors and thermistors made of diamond may be attached as integral parts of other active and passive diamond devices.

The high dielectric strength of diamond combined with its acceptable dielectric constant of 5.61 and low mass render diamond the capacitor of choice for the highest charge storage density per unit weight. The figure of merit for use as a capacitor is further improved by virtue of its low loss tangent of $6x10^{-4}$. Even better, the loss tangent change with temperature is negligible up to 550° C. The dielectric constant itself increases with temperature at approximately 1% per 100° C.[8] Unlike reverse biased capacitors made in other conventional semiconductors, capacitors made in diamond exhibit negligible leakage – even at temperatures of 300° C and higher.

Printed Circuit Boards

Traditional design of massive high performance digital logic circuitry incorporates "mother boards" that serve to interconnect the signals passing among all of the logic circuit boards. In supercomputers and related applications these individual logic boards and memory boards are individually cooled on their undersides by liquid heat exchangers. This arrangement limits the stacking density of the individual circuit boards thus increasing signal path delay and setting limits on overall processing speed. The use of diamond as the "boards" for mounting the integrated circuits enables a new physical architecture that provides for significantly shorter signal paths. Polycrystalline diamond "slabs" of a mm thickness have recently been developed at several facilities. This material is known as white diamond (by virtue of its color). These "slabs" exhibit thermal conductivities between 17 and 20 W/cm-°C and can serve as printed circuit boards (PCBs) for the mounting of silicon integrated circuits. With thermal conductivities greater than 10 times that of the best previous PCBs, edge cooling can be employed. This not only permits a much greater stacking density of the individual PCBs, but (by removing the cooling from the underside of each PCB) enables the elimination of the motherboard for signal routing. Overall volume can be reduced by a factor of 6, weight can be reduced by a factor of 4, and operating speeds of 350% of present technology are envisioned.

The thermal coefficient of expansion of diamond at 1.1×10^{-6} is lower than that of silicon at 2.6×10^{-6} or GaAs at 5.9×10^{-6}. It is even lower than that of invar over a wide temperature range. A cursory observation may indicate that this is much too low to be compatible with silicon or GaAs. Two points are in order, however. First, the temperature rise of the IC chips mounted on diamond will be much lower than would otherwise occur and second, both silicon and GaAs ICs can be mounted to smooth diamond by VanderVaals bonds.[9] The process is referred to as topotaxy. With such an attachment, the ICs can accommodate a small lateral movement, but vertical movement and thermal conductivity are not affected. Using such bonding, thin epitaxial films have actually been attached, ion implanted, and subsequently annealed without experiencing failures of any kind.

The use of diamond substrates for thermal heat extraction coupled with their insulating low loss tangent qualities and their intrinsic capability to be used as resistors and capacitors as well renders them very versatile as PCBs.

Integrated Circuits

Integrated circuits of diamond, while feasible, await several technological advances. The first is a single crystalline diamond substrate of at least 2" in diameter such that it can be handled in automated processing equipment. Since single crystalline diamond films are as yet grown only on diamond and natural diamond is not available in these dimensions, and artifact diamond boules in these dimensions do not currently appear to be feasible, diamond ICs will be some time away. To circumvent this non-availability problem, two basic pursuits are underway. First, the heteroepitaxial nucleation and growth of diamond on foreign substrates is being pursued. To date, these have not proven successful – even though there have been claimed successes on copper. Second, it has been noted that small diamond particles physisorbing to a smooth surface always align with their {111} axis normal to that surface. "Checkerboard" patterns of very small anisotropically etched "holes" have been created in {100} silicon and these holes subsequently were filled with single diamond particles self-oriented such than the diamond {100} axis is aligned with the silicon {100} axis. These oriented diamond particles were subsequently overgrown with an artifact diamond film that coalesced with low angle grain boundaries of approximately 0.2 degrees.[2]

In this manner large area (e.g., 1" x 0.5") "single crystal" diamond films have been grown that exhibit x-ray rocking curve patterns similar to those of many natural diamonds.

The fabrication of diamond integrated circuits has many features to its advantage. First among these is that diamond is the strongest of all materials; it is very difficult to break a 40 mil thick diamond film. Second, it would be virtually impossible to accidentally scratch the diamond film during processing. Third, a hydrogen passivated diamond surface would be immune from any environmental attack at temperatures below 600° C. Fourth, diamond is transparent; any flaws/defects are clearly observable with a microscope. Finally, diamond can be etched with precision greater than that available to any other semiconductor material.[10] Just as with the use of diamond as a PCB, diamond ICs could contain resistors and capacitors as well as the active devices.

Non-Volatile RAMS

Recently it has been shown that pseudo non-volatile dynamic RAMs may be made in GaAs using reversed biased p-n junctions of GaAs as the memory storage cell and that R.T. refresh time can be on the order of an hour. Since this memory storage time is exponentially related to the bandgap, an incentive exists to utilize higher bandgap materials.[11,12] This citation describes 3 hours storage in SiC devices at 160° C. With diamond, the storage times could be much longer and/or the operating temperatures much higher.

Radiation Hard Technology

The low capture cross section of carbon to neutrons combined with the very strong C-C bond binding energy renders diamond **the** prospective semiconductor material of choice for immunity to radiation damage. Although extensive testing still remains, preliminary radiation exposure tests of discrete diamond devices indicate that diamond devices will be extremely radiation hard.[2]

Inhibiting Factors

There are several factors currently inhibiting the use of diamond semiconducting devices and ICs. First among these is that there is no known shallow substitutional donor that can be used in the ranges of greatest usefulness. Substitutional nitrogen is a deep donor some 2 eV beneath the conduction band minima and is therefore detrimental. Both lithium and sodium are interstitial shallow donors. Sodium is too large to exhibit large diffusivities and even lithium is a comparatively slow diffuser in diamond. Their problem, however, is that as substitutional impurities, they are acceptors! Their site location can not, as yet, be adequately controlled. Carbon, when implanted at a fluence exceeding $10^{15}/cm^2$, results in N+ activity. While this renders it useful for source and drain ohmic contacts, it can not be used for active channel implants at lower concentrations; its efficacy as a donor may be related to defects. A prospect for donor activity in diamond derives from heterojunction injection from a higher bandgap material such as lattice-matched cubic boron nitride (cBN). If such prospects materialize, then high electron mobility transistors (HEMTs) of diamond may result.

Acceptor activity in diamond is also not without problems. Substitutional boron is a known acceptor, but with an activation energy of approximately 300 meV. Degenerately boron doped diamond exhibits a much lower activation energy. Heterojunction injection from cBN also appears to be a viable approach to p channel devices.

Biography

Mr. Max Yoder is an electronics engineer with the Solid State Electronics Branch of the Office of Naval Research where he supervises programs in semiconductor materials, monolithic microwave integrated circuits, gigabit logic, new electronic device structures, and electromagnetic system applications . He has published and presented many papers in these fields of solid state materials. He is a pioneer in the development of research programs for monolithic microwave devices and wide bandgap semiconductors in the U.S. Currently he manages at ONR the new research program in diamond semiconductor technology.

References

1. Private communication, Dr. B. Pate, Washington State University.
2. Private communication, Dr. M. Geis, M.I.T. Lincoln Laboratories.
3. M. Kordesch, *Electronics Letters*, in press.
4. A. Johnson, *RCA Review* **26**, 163 (1965)
5. R. W. Keyes, *Proc. IEEE* 60, 225 (1972.
6. Private communication, Prof. R. Trew, N.C.S.U.
7. A. M. Goodman and A. Rose, *J. App'l Phys.*, Vol 42 No. 7, p 2824, June 1971.
8. Information on the dielectric properties of diamond were provided by Rockwell International.
9. E. Yablonovitch, et al, *App'l. Phys. Ltr.*, Vol 56, p 2419 (1990).
10. M. Yoder, U.S. Patent #4,756,794.
11. P.G. Neudeck, J.S. Kleine, S. T. Sheppard, B.T. McDermott, S.M. Bedair, J.A. Cooper, Jr., and M.R. Melloch, "Electrical Characterization of GaAs PiN Junction Diodes Grown in Trenches by Atomic Layer Epitaxy," *Applied Physics Letters*, Vol. 58, pp. 83-85, 7 January 1991; and, T. B. Stellwag, J.A. Cooper, Jr., and M.R. Melloch, "A Vertically-Integrated GaAs Bipolar DRAM Cell,"

1991 IEEE Device Research Conference, Boulder, CO, June 17-19, 1991.

12. C. T. Gardner, J. A. Cooper, Jr., M. R. Melloch, J.W. Palmour, and C. H. Carter, Jr., "Electrical Characterization of PiN Diode Structures in 6H-SiC," 4th Int'l. Conference on Amorphous and Crystalline Silicon Carbide and Other IV-IV Materials (ICACSC ;91), Santa Clara, CA, Oct. 10-11, 1991.

Profiles in Science

Dr. Rustum Roy

Dr. Rustum Roy, the Evan Pugh Professor of the Solid State at The Pennsylvania State University, is one of the nation's leading materials scientists, specializing in the synthesis of new ceramic materials. For 42 years, he has been a principal investigator of the Office of Naval Research (ONR), and his work spans the field of both new materials and processes. His most renowned research is in the areas of hydrothermal and high pressure anvil processes; perovskites, synthetic clays and zeolites; low expansion ceramics, and diamond films. Dr. Roy is founder and director of the Pennsylvania State University's Materials Research Laboratory, where he started diamond research 25 years ago. Today, his laboratory conducts one of the nation's largest efforts in diamond research.

In 1948, as a postdoctoral student under Professor E. F. Osborn with funding from ONR, Roy was instrumental in the discovery of the sol-gel process which is now a substantial branch of ceramic science, leading to the development of hydrothermal phase equilibria and processing science and the design of vital research equipment in the field.

In 1957, when Professors Roy and Tuttle extended the hydrothermal pressure range to high pressure Bridgman anvils from 5 kbars to 200 kbars, they became pioneers in diamond research, again with ONR support.

As a principal investigator for ONR, Professor Roy brought diamond film research to the U.S. Recently Roy discovered a new technique for making synthetic diamonds which promises a simple and cheaper route to the production of bulk diamond and diamond composite objects. The process is titled low-pressure, solid-state-source synthesis of diamond which operates at atmospheric pressure and uses solid state sources of carbon as distinguished from traditional chemical vapor deposition (CVD) process.

Diamond Chemical Vapor Deposition*

F. G. Celii
Texas Instruments, Inc. Central Research Laboratories, Dallas, Texas
J. E. Butler
Gas/Surface Dynamics Section, Naval Research Laboratory, Washington, D.C.

1. Introduction

Diamond, the hardest of all materials, has captivated civilizations for many centuries.[1] The allure of diamond is no less strong today, although for different reasons. Diamond possesses many attractive material properties,[2] besides hardness, which motivate technological interest. These extreme properties, as well as the relative scarcity and inherent high cost of natural stones have severely limited application, thus stimulating research into synthetic methods of diamond production.

The first successful synthesis of diamond on a commercial scale occurred in the mid-1950s; high pressure, high temperature (HPHT) techniques were used, in which diamond is produced by recrystallization of metal-solvated carbon at 50-100 kbar pressure and 1500-2000 C.[2-6] Of the industrial diamonds consumed in 1990, HPHT diamond accounted for more than 90% (60 tons).[7] Efforts to produce diamond directly from gases proceeded in parallel with development of HPHT processes; Diamond could be synthesized under metastable conditions-temperatures and pressures (≤1 bar) at which graphite is the thermodynamically-favored form of carbon.[8] Vapor-phase diamond growth remained a laboratory curiosity, however, because of extremely low deposition rates. Significant advances[4-11] in the early 1980s brought about growth rates in the range of micrometers/hour (μm /hr) and refocused attention on the synthesis of diamond by chemical vapor deposition (CVD). The potential for economic scale-up of diamond CVD processes suggested an alternative to HPHT production for diamond abrasives or heat sinks. In addition, the important new potential of coating the large-area surfaces with diamond may remove the traditional restrictions on the use and application of diamond. This capability has stimulated active research into all aspects of diamond CVD.

Scientific interest in diamond CVD processes stems not only from the potential applications, but also from the need to explain the improbable growth of diamond under apparently metastable conditions. At room temperature and pressure, graphite is the stable form of solid carbon: Although the enthalpy of graphite is a mere 2 kJ /mole lower than diamond, extreme conditions are necessary to surmount the barrier for inter-conversion of the two carbon allotropes. Indeed, the combination of strong sp^3 bonds [C-C bond strength of 389 kJ/mole[12]] and the highest volumetric atom density of any known material is responsible for many of the superlative

* *This review was originally published in the* Annual Reviews of Physical Chemistry, *1991, vol. 42, pp. 643-684. For a paper focussed on the mechanisms of diamond growth, "Thin film diamond growth mechanisms" by J.E. Butler and R.L. Woodin will appear in* Phil. Trans. Roy Soc. London *in early 1993.*

properties of diamond. Several aspects also make understanding of the diamond CVD mechanism a potentially solvable research problem. For instance, there is a large body of combustion literature, which provides basic reaction rate data for many hydrocarbons and can lead to an understanding of the gas-phase species involved in diamond CVD processes. Also, the symmetric cubic structure of the bulk diamond lattice and the small number of electrons associated with carbon make the theoretical calculation of surface and gas-surface interactions tractable. Finally, relatively simple and widely-available analytical techniques for diamond analysis, such as Raman scattering, scanning electron microscopy (SEM), and x-ray diffraction, allow universal and unambiguous comparisons of material produced in different laboratories.

The many potential applications of CVD diamond are feasible because the diamond produced by CVD methods is comparable in purity and properties to HPHT or natural diamond. The hardness of diamond, coupled with the conformality of CVD films, can be exploited to make tool coatings and inserts with long cutting lives. Diamond could provide protective windows or optical coatings with high transmittance in the visible and infrared (IR), although the production of optical-quality diamond is currently difficult (Figure 1a). The polycrystalline nature of CVD diamond films often yields rough surfaces (Figure 1b), which require polishing for numerous applications. Thin diamond membranes (Figure 1c) are also transmissive to x-rays and may be used as shadow mask supports for x-ray lithographic fabrication of electronic devices. The rare combination of high thermal conductivity, electrical resistivity, and breakdown voltage makes diamond well-suited for thermal management applications in electronic packaging. Polycrystalline diamond plates possess thermal conductivity ~2.5 times that of copper at room temperature [single-crystal diamond is a factor of 2 still higher[2]]. With a coefficient of sliding friction equivalent to Teflon, smooth diamond surfaces could also have many tribiological applications. Semiconducting diamond (produced by doping) with a 5.5 eV bandgap and high electron and hole mobilities, holds promise for high-temperature, high-speed power devices[15,15a]. The single crystal diamond needed for electronic device applications can also be produced by CVD methods (Figure 1d).

Advances in diamond growth rate have generally stemmed from improved methods of gas-phase activation.[9-11] Numerous activation or carbon-transport techniques, including thermal (hot filament) or plasma (dc, rf, microwave) activation, electron-enhanced or ion beam deposition, laser ablation, and combustion flames, have all been explored for diamond production at pressures of 1 atm or less. Deposition rates in the range of 0.1 to several μm/hr have been typical. There is some commonality of parameters between many of the techniques, e.g. substrate temperatures in the 1100-1400 K range and the carbon source gas diluted in H_2 (typically <2%). Nucleation using diamond abrasion is a common procedure and an active area of research. The deposited material may contain mixtures of carbon with various bonding (sp^2 and sp^3), structural (crystalline vs. amorphic), and compositional (C-C vs. C-H) forms. Recently, diamond growth rates in excess of 300 μm/hr or deposition areas of >200 cm^2 have been demonstrated by using plasma jets or atmospheric pressure combustion torches.

Although high-quality diamond can be routinely produced by using a myriad of techniques, our understanding of the deposition mechanism is far from complete. As with any CVD technique, diamond CVD involves many component gas phase and surface processes (Figure 2). Gas-phase reactions may be driven by thermal, plasma, or combustion activation to produce reactive products. Once generated, transport of the gaseous species to the substrate occurs by some combination of laminar, convective, and diffusive flow, with reactions continuing to modify relative concentrations. With moderate pressure techniques, movement of species into and out of a boundary layer may control the gas-phase environment above the growth surface. Adsorption and the desorption processes couple the gas phase reactions to those at the surface. Diffusion along the growth surface eventually leads to diamond crystal nucleation and growth, whereas diffusion of material into the bulk may compete with the growth process. In the following

Figure 1.

Examples of CVD diamond: (a) Free-standing piece of transparent polycrystalline CVD diamond grown using a dc torch.[13] The sample is 55 μm thick and 16 mm diameter. (Courtesy of P. Klocek, J. Hoggins, and T. McKenna, Tex. Instrum.) (b) SEM of polycrystalline diamond surface deposited with a microwave CVD reactor. (c) Free-standing diamond membranes (~2-3 μm thick) on 50 mm and 25 mm Si supports. (d) Homoepitaxial diamond grown on a natural diamond seed using an oxy-acetylene torch.[14] (Courtesy of K. Snail and L. Hanssen, Naval Res. Lab.

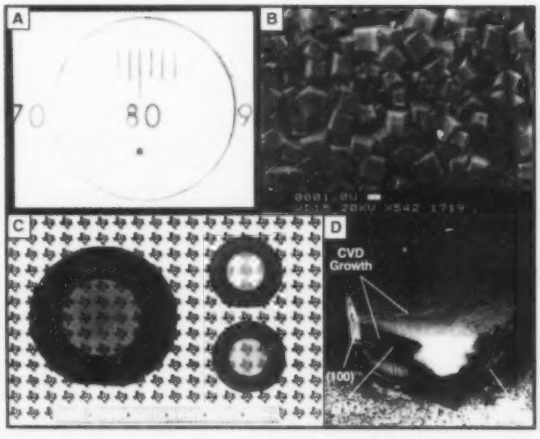

sections, we assemble the information available on each of the component CVD mechanisms.

There are several recent reviews on diamond[4-6,8,16-22] and diamond-like carbon (or, hard carbon)[17, 18, 23, 24] deposition processes. In this review, we focus specifically on the chemical mechanisms and surface physics relevant to CVD diamond growth. The nature of diamond surfaces is first described in Section 2. The related issues of nucleation and surface growth processes are then examined in Section 3. Finally, our understanding of the gas-phase chemistry is summarized in Section 4 and combined with models of diamond growth mechanisms in Section 5.

2. Diamond Surface Studies

The nature and structure of the diamond surface determines how the crystal interacts physically and chemically with the rest of the world through friction, wear resistance, adhesion, chemical corrosion, and electrical conduction. The interfacial properties are affected by the surface species, the atomic arrangement, and the associated electronic density of states. Relevant to the CVD deposition process, diamond growth also depends sensitively on the nature of the crystal surface. In this section, we review diamond surface properties and place particular emphasis on single-crystal surface studies, as these present simplified pictures to explain polycrystalline diamond growth.

Figure 2.

A schematic of the diamond CVD process. Various reactive and transport processes are shown in the gas-phase and surface. Diffusion through a boundary layer (dashed line). and into the crystal bulk (B) are also depicted.

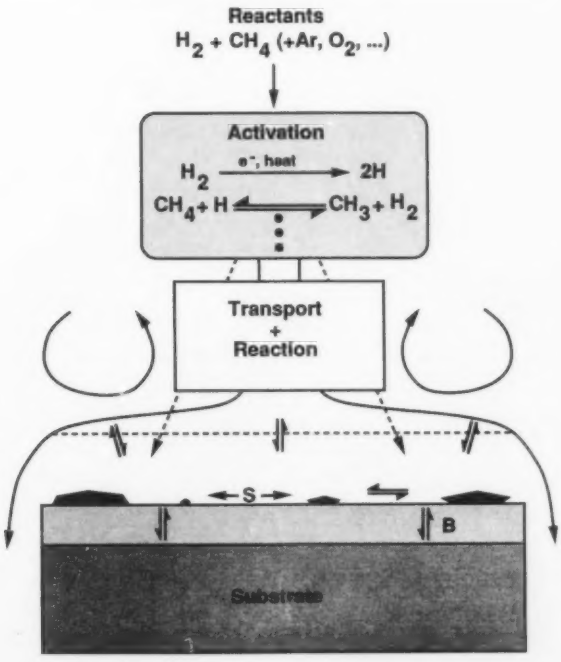

2.1 Properties of Diamond Surfaces

Many diamonds are hydrophobic, a property which is exploited in diamond mining for recovery of natural stones: Diamond is separated from an aqueous slurry of ore by adhesion to greased tables and belts.[1] In this respect, diamond can be viewed as a large carbon core surrounded with an alkane coating, which results from hydrogen termination of the crystalline lattice. Diamond surfaces prepared by polishing in oil are hydrophobic, as are halogenated surfaces.[25,26] Hydrophilic behavior can be induced through oxidation at elevated temperatures[26] or by treatment with alkaline detergents.[27,28] Heteroatoms detected on the surfaces of diamond powders and crystals are principally H and O, although F and Cl can be observed after treatment in halogen-containing discharges or concentrated HCl.[26] The presence of CH_2, CF, CO, and C-O-C functional groups have been detected by IR spectroscopy after various chemical treatments.[25,29]

Atomically "clean" diamond surfaces require ultrahigh vacuum (UHV) conditions and crystal temperatures in excess of 1300 K.[30] Thermal desorption of H_2 from hydrogenated diamond powders occurs between 900 and 1500 K, with two principal desorption peaks at 1200 and 1500 K.[31] Oxidized powders desorbed CO and CO_2 over 300-1300 K, with CO_2 desorption peaked at 730 K and CO at 890 K.[32,33] Above 1000 K, the desorption is due to CO.

The preparation of oriented single crystal diamond for surface studies is not trivial. Single crystal diamond cleaves most readily to leave (111) crystallographic faces. Other cleavage planes are seldom encountered in natural stones because of their higher cleavage energies.[2] Diamond surfaces can be cut by using diamond-impregnated disks and polished by abrasion with diamond powder loaded into a cast iron wheel (scaife) or high-speed lap.[34-37] Polishing rates can vary by several orders of magnitude, depending on the crystal face.[2] By viewing the polishing process as a microscopic "chipping-away" of surface material, one might expect that while the macroscopic orientation of the polished surface may be (100) or (110), the exposed microscopic surfaces could contain small planes of (111) orientation. This issue could complicate the interpretation of experiments on nominal (110) or (100) surfaces. However, distinct growth rates and surface morphologies observed for diamond CVD on the individual diamond faces (see Section 3.1) imply that true (110) and (100) planes are prepared.

2.2 The (111) Diamond Surface

The most studied surface of diamond is the (111) cleavage surface. Pate[38] provided an excellent summary of the atomic and electronic structure of the (111) surface. Numerous spectroscopic techniques have been enlisted to study diamond surfaces. For instance, Auger electron spectroscopy can distinguish diamond bonding from that of graphite or carbides by use of the carbon KVV signature.[38-40] Low-energy electron diffraction (LEED)[30, 38, 41-46] and He scattering[47, 48] indicate that the as-polished surface has the structure of the ideal (111) bulk-terminated diamond lattice. However, the 1 x 1 LEED pattern (repeat structure of one unit cell by one unit cell) is indistinguishable from the (0001) plane of graphite.[38] Upon annealing above 1000° C in UHV, half-order diffraction spots appear, indicative of a 2 x 2, or multidomain 2 x 1, surface reconstruction.[38, 43] The reconstruction provides further evidence that the surface is not a graphite structure.

The diamond interface characteristics are a sensitive function of surface conditions. The as-polished (111) surface exhibits no electronic states within the bandgap of diamond[49, 50] and has high resistivity and a low friction coefficient;[51] the reconstructed surface had occupied and unoccupied states in the bandgap,[49-54] is electrically conductive, and has a high friction coefficient toward an atomically-clean metal surface.[51] Photon-stimulated ion desorption (PSID) of H^+ ions reveals that the 1 x 1 surface is hydrogen-terminated, whereas the reconstructed surface is hydrogen-free.[55] Exposure of the annealed surface to hydrogen excited by a hot filament (generating H and/or H_2^*) removes the bandgap states and returns the friction coefficient to its original value.[51] There is also evidence that electron and ion bombardment of the surface produce surface graphitization and electronic states in the bandgap.[50] High-resolution electron energy loss spectroscopy finds vibrational resonances characteristic of -CH and $-CH_3$ on the as-polished surface, but $-CH_2$ resonances were not detected on the reconstructed surface.[52, 56]

Several models[57-60] have been proposed for the structure of the 2 x 2/2 x 1-reconstructed (111) surface of diamond and silicon.[38] Theoretical calculations[61-65] have examined and refined Pandey's[58] π-bonded chain model. Quantitative analysis of the C KVV Auger line-shape provides evidence for antiferromagnetic spin ordering, consistent with the π-bonded chain model of the (111)-(2 x 1) reconstructed surface of diamond.[66] Comparison of experimental data[38, 44, 67] on surface energies and dispersion of electronic states of the reconstructed surface with the theoretical calculations[61-65] likewise support the Pandey model, with recent evidence for a relaxed π-bonded chain model of the reconstruction.[67]

Aside from the reactions of the (111) reconstructed surface with H and H_2, there are few studies of interaction with other gases. The clean (111) surface is unreactive to O_2, N_2, NH_3, and H_2S, whereas evaporated Al produces aluminum carbide upon high temperature annealing.[43] The reaction of NO with the (111)-2 x 1 surface is slow, with a sticking coefficient of ~10^{-8}, but can be enhanced by more than 100 times by surface excitation with above-bandgap laser irradiation.[68] There is some evidence for $-CH_3$ groups on the (111) surface,[56] but theoretical calculations indicate that high $-CH_3$ coverages would result in significant strain because of the close proximity of the surface carbon bonding sites.[69] Other atomic adsorbates have been detected, principally oxygen[50] and halogens.[70, 71] The low coverages of nonhydrogen adsorbates is presumably due to the steric hinderance on the densely-packed surface.

Figure 3.

Models of diamond surface structures: (a) Dihydride-terminated (100) surface; (b) Monohydride-terminated (100)-(2x1) reconstructed surface; (c) Diamond (100)-(2x1) π-bonded surface. (From Ref. 76, with permission.)

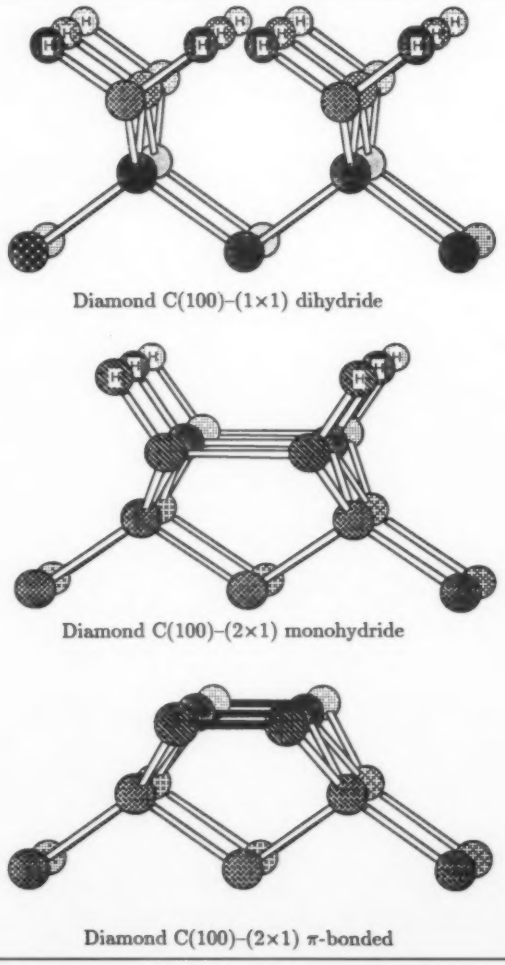

Diamond C(100)–(1×1) dihydride

Diamond C(100)–(2×1) monohydride

Diamond C(100)–(2×1) π-bonded

An intriguing property attributed to the (111) surface of diamond is a low,[50, 72] and possibly negative,[74] electron affinity, which could lead to potential applications of diamond as a cold cathode emitter.[74]

2.3 The (100) Diamond Surface

Few experiments[38, 42, 75, 76] have been performed on the diamond (100) surface. The dihydride-terminated bulk structure is expected to be distorted from a normal sp^3 geometry, because of steric interactions between the hydrogens [assuming normal tetrahedral bonding angles and the C-H bond length of 1.09 Å determined for the (111) surface,[47] a H-H spacing of 0.63 A is derived vs. 0.74 Å for gaseous H_2]. As with the diamond (111) surface, LEED studies of the as-polished surface indicate a structure indistinguishable from the bulk (1 x 1 pattern), and half-order diffraction spots appear after annealing above 1300 K, which indicated a superposition of 2 x 2 and 1 x 2 structures.[43] Unlike the (111) surface, the reconstructed (100)-2 x 1 retains partial hydrogen coverage even after annealing to 1430 K in UHV.[76] Also, carbon-containing ions were observed in PSID experiments, unlike the (111) surface, which yields only H^+. Two distinct time-of-flight distributions are observed from the electron-stimulated desorption of H^+, with the faster component of the H^+ distribution disappearing at the onset of the 2 x 1 reconstruction.[76] Hamza et al[76] have proposed that the 2 x 1 reconstructed surface is a monohydride termination of dimer pairs (Figure 3).

Thermal desorption measurements from the as-polished (100) surface yield up to ten monolayers of hydrogen and indicated the presence of hydrogen in the near-surface bulk region, as well as on the surface.[76] Large concentrations ($\leq 5\%$ by volume) of bulk hydrogen have also been detected in polycrystalline CVD diamond films by using nuclear resonance reaction analysis.[77] At low hydrogen surface coverage, desorption is first order with an activation energy of ~37 kcal/mole and a pre-exponential factor of $\sim 3 \times 10^5 s^{-1}$. Similar to the (111) surface, occupied states are observed in the band gap for the 2 x 1 reconstructed surface, but not for the 1 x 1 unreconstructed surface.[76]

2.4 The (110) Diamond Surface

The diamond (110) surface is the least-studied of the low index planes. The as-polished surface exhibits a 1 x 1 LEED pattern consistent with the structure of the truncated bulk; however, unlike the (111) and (100) surfaces, no reconstruction is observed after annealing to over 1300 K.[43] The PSID yield of H^+ decreased by three orders of magnitude when the surface was heated from room temperature to more than 1400 K, which indicates a hydrogen termination of the as-polished surface and a "clean," but unreconstructed, high-temperature surface.[38] Tensiometric studies of surfaces after high temperature reaction with oxygen determined that the (110) surface of diamond is significantly more hydrophilic than the (111) face with a maximum coverage of 0.3 monolayer presumed to be in the form of -OH groups.[28] Exposure to F and F_2 saturates at 0.8 and 0.2 monolayer coverage, respectively.[78]

2.5 Diamond Surfaces and Diamond CVD

Under conditions of diamond CVD, heated surfaces are exposed to atomic and molecular hydrogen, as well as various hydrocarbon species. The structural information regarding the interaction of hydrogen with diamond surfaces can be summarized as follows. The cleaved diamond (111) surface is terminated with C-H bonds and retains the bulk structure. Annealing the surface to more than 1300 K in vacuum produces a hydrogen-free surface that reconstructs to form ordered 2 x 1 domains of π-bonded chains, and reversibly adsorbs atomic hydrogen to revert back to the 1 x 1 hydrogen-terminated surface. The structure of the unreconstructed diamond (100) surface appears to be a strained dihydride termination of the surface carbon atoms, whereas the 2 x 1 reconstructed surface is thought to be a monohydride termination of dimer pairs. The picture for the diamond (110) surface is far more speculative, with the as-polished surface presumed to be hydrogen-terminated and the annealed surface hydrogen-free, but not reconstructed. These observations indicate that diamond surfaces are largely terminated with C-H bonds under CVD conditions. The lifetime and concentration of surface radical sites generated by hydrogen removal would depend upon the balance of temperature-dependent H and H_2 desorption, adsorption, and abstraction rates, as well as the adsorption rates of relevant hydrocarbon species.

3. Nucleation and Surface Growth Processes

There are two distinct, yet related, issued in the heterogeneous growth sequence of diamond: nucleation and surface growth processes. An understanding of the growth mechanism on diamond surfaces is necessary to explain the variation in rate and surface morphology observed for deposition on the low-index faces of diamond. Chemical vapor deposition diamond growth on diamond surfaces is also relevant for deposition on nondiamond substrates: Following the nucleation of diamond crystallites, the competitive growth on various faces can help determine the poly-crystalline film properties. The initial step of nucleation on nondiamond substrates is an area of importance that has bearing on adhesion, film properties, and the type of substrates that can be successfully coated.

3.1 Diamond Growth on Diamond

Many early studies of diamond CVD employed the weight gain of diamond particles to determine deposition rate (see Section 4.5). Investigation of homoepitaxial growth, i.e. diamond deposition on diamond single-crystals, was only

recently reported.[79-84] The diamond growth rate decreased in the order (111)≈ (110)>(100) in a microwave plasma CVD reactor, and planar growth on (100) was particularly sensitive to temperature.[79] Recent filament[80, 81]- and microwave plasma-assisted[82-84] deposition studies found a similar order of growth rate, (110)>(111)>(100)[4.1, 1.8, and 1.3 μm/hr, respectively[80]]. Smooth, stress-free films are observed only on the (100) face,[80-84] whereas films deposited on (111) faces have a high defect density and crack spontaneously to relieve stress.[81, 82] Doping with boron during deposition significantly alters both the growth rates and resultant film morphologies. Growth rates of 14, 6.6, and 0.7 μm/hr are measured for the (110), (100), and (111) faces, respectively.[80] Smooth, boron-doped films are prepared on (100) and (110) faces, while highly-defective, twinned films are deposited on the (111) face. The homoepitaxial growth studies are particularly significant for the application of diamond in active electronic devices.

3.2 Nucleation on Nondiamond Substrates

Unlike homoepitaxial diamond growth, diamond deposition on almost all nondiamond materials is impeded by the lack of nucleation. Nondiamond surfaces are frequently seeded with diamond particles to enhance nucleation and initiate growth. Consequently, there has been much work directed toward understanding the diamond nucleation phenomenon. The development of alternative nucleation approaches has been vigorously pursued because of its technological importance.

Real-time monitoring during the early stages of diamond deposition would enormously aid our understanding of the growth mechanism. As we discuss below, much of our current information comes from postgrowth film analysis. In situ surface studies are far less common than gas-phase measurements (see Section 4), because the growth pressures are high enough to preclude most traditional surface science techniques. Optical diagnostics, such as IR absorption,[85] would be useful in this regard, but have not yet been reported for diamond CVD systems.

Nucleation is most commonly assisted by abrasion or seeding[85a] with diamond powder. Diamond abrasion reduces the induction time for nucleation and increases the nucleation density.[86] Many hard materials (e.g. BN, SiC, Al_2O_3) may be used to abrade and damage substrate surfaces; however, diamond has the most significant effect on promoting nucleation[86][although cubic boron nitride (c-BN) and SiC[87, 88] were also reported to enhance nucleation]. Because surface ledges,[86] or other morphology,[89] were not effective in promoting diamond nucleation on nondiamond surfaces, imbedding of diamond particles is considered the dominant mechanism. The nucleating effect of diamond abrasion can be decreased by using ultraviolet (UV) laser light,[90] presumably by graphitization or coverage of the diamond seeds. Recent observation[91] of ~100 nm diamond flakes, which cover a diamond-abraded surface, strongly suggests that imbedding is indeed responsible for nucleation by promoting diamond-on-diamond growth. It has also been proposed that surface defects[92] or pseudomorphic lattice matching[93] reduce the free energy of diamond, compared with graphite, and thus stabilize the nucleation of diamond.

Lux and coworkers[94, 95] have studied the nucleation and growth of diamond on various metallic substrates. By using both clean[94] and diamond-impregnated[95] substrates, they determined the nucleation density, growth rate, and interfacial layer thicknesses from stop-growth experiments. The results were interpreted in terms of carbon diffusion rates into the substrates that control the steady-state carbon supersaturation at the surface. The induction times for nucleation are shortest for those metals with low carbon diffusion rates (e.g. Hf, Nb, Mo).[94] The enhanced nucleation observed at the interface of diamond-impregnated metals likewise indicates the promoting effect of high surface carbon concentration.[95] The diffusion rates also affect crystal growth; lower bulk diffusion rates allow larger crystal sizes to be formed, presumably because of increased surface diffusion.[94] These results indicate that substrates that can absorb carbon into the bulk, often by forming carbides, delay diamond nucleation.

An understanding of diamond nucleation has been sought through investigation of the substrate/diamond interface. Metal carbides were identified by x-ray diffraction at various metal/diamond surfaces,[94, 96] but the relative thicknesses of the carbide layers did not correlate with the carbon diffusion coefficients of the metals. The large difference in Mo_2C layer thickness produced by microwave plasma-assisted growth[97] and filament-assisted CVD[94](1.5 μm and 16 μm, respectively) indicates a dependence of Mo_2C formation on the exact growth conditions, and not simply the carbon diffusion characteristics. Following diamond CVD growth on Si, a SiC interfacial layer was detected by using IR absorption,[97] transmission electron microscopy,[98-100] and ellipsometry.[101] The SiC layer thickness decreased as the initial CH_4/H_2 ratio increased from 0.3 to 1.0%[97], and the SiC layer could not be detected in samples deposited at 2% CH_4/H_2.[98-100] The SiC layer thickness was 40-70 Å for microwave plasma growth at 0.5% CH_4/H_2 conditions.[101] Williams et al[100] suggested that significant diffusion of carbon into Si occurs under low methane concentration, whereas the surface is "capped" at the 2% CH_4/H_2 growth conditions. Also, the SiC interface prepared by microwave-assisted growth has been identified as crystalline β-SiC,[98-100] while an amorphous SiC layer was found in the case of biased filament-assisted deposition.[102] Deposition on Si may be a special case, as Badzian et al[103] have proposed that elemental Si plays a catalytic role toward promoting nucleation.

Belton and coworkers have performed x-ray photoelectron spectroscopy (XPS) of filament-assisted diamond deposition on Si,[104] Ni,[105] and Pt.[106, 107] Unlike other stop-growth experiments, the samples remained under vacuum, which

Figure 4.

Characterization of diamond growth on Si from the time dependence of XPS spectra in the C (1s) region. The initial surface carbon contamination, the formation of a SiC layer, and diamond film growth are observed (From Ref. 104, with permission.)

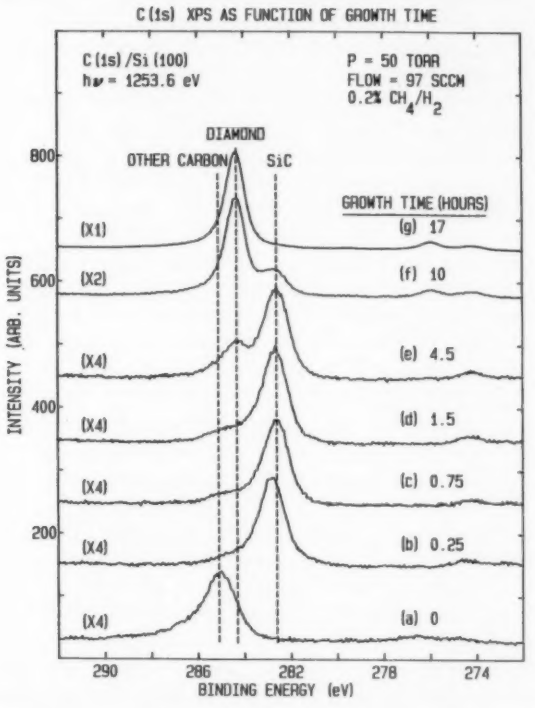

allowed intermediate stages of growth to be analyzed. For deposition on Si, the initial surface appeared to be carbon-covered SiO_2. A SiC layer was formed following 15 minutes of deposition, which was later overgrown by diamond (Figure 4). From LEED studies,[105] it was determined that carbon deposition on Ni proceeds through various stages: An ordered carbon overlayer is covered by microcrystalline graphite, then glassy carbon, before diamond crystals start to form. On Pt foils, graphitic islands were converted to adsorbed hydrocarbons. A continuous diamond film grew over the diamond-scratched foil, whereas coverage of the unscratched foil was incomplete. Although it was possible to resolve separate contributions from species on Si in the C(ls) XPS spectra, the energy shifts of carbonaceous species on Ni and Pt are much more subtle and can only be extracted by curve-fitting. Electron energy loss spectroscopy (EELS) has been applied to diamond growth on Si and Ni,[107, 108] but the EELS spectra could not be quantified as readily as XPS.

The interface studies have been quite important for insight into surface species present during growth, but it has not been possible to establish their relevance to the nucleation mechanism. For instance, were the graphitic islands present during growth on the Pt surface[106, 107] necessary nucleation sites for diamond, or simply a competitive carbon deposition channel? Do the carbide layers detected on various surfaces play an active role in the nucleation step? In the case of growth on Si, the final SiC layer thickness is achieved in only ~2 min, long before diamond nucleation occurs,[101] which indicates that carbide formation is not a necessary condition for subsequent diamond growth, but a competitive carbon reaction channel. Nonetheless, the presence of the carbide layer may affect adhesion. Imaging techniques, such as scanning tunneling microscopy[109] and atomic force microscopy, may help resolve these nucleation issues.

Hartnett et al[110] have investigated the effect of various deposited intermediate layers on the diamond nucleation density. Although SiC is detected at the diamond/Si growth interface,[98-102, 104] a deposited SiC layer on Si resulted in no nucleation enhancement. A boron nitride layer containing ~30% c-BN increased nucleation by a factor of 40. The heteroepitaxial growth of diamond on c-BN, which was anticipated because of the close match between the two lattices (c-BN: 3,616A; diamond: 3.567A), was recently reported.[111, 112] Because c-BN is itself a difficult material to produce at present, heteroepitaxial diamond growth on c-BN does not offer an inexpensive or convenient alternative to homoepitaxial growth on diamond substrates.

The use of carbonaceous intermediate layers has been a promising approach for promotion of diamond nucleation. Diamond growth on an amorphous hydrogenated carbon (a-C:H) film was attempted, but the layer was etched under diamond CVD conditions and did not enhance nucleation.[110] A laser-ablated carbon film, however, increased the nucleation density by a factor of ~40.[110] Nucleation density enhancement using carbon-rich oxy-acetylene torches was also reported.[87, 88] Accelerated nucleation resulted from carbon layers deposited following pump oil application to abraded surfaces.[113] The decrease of nucleation induction time in these cases[87, 88, 113] is thought to result from rapid carbide formation and carbon saturation at the substrate surface.

It may be naive to assume only a single mechanism for diamond nucleation. Diamond synthesis has been reported in which homogeneous gas-phase nucleation was invoked.[114] Ion-beam deposition of diamond on Cu substrates was also recently reported.[115] [Diamond growth on Si[16] was later retracted.[117] Analysis of the fine grains[114] and thin layers[115-117] is difficult because definitive techniques, such as Raman scattering, cannot be employed.] Diamond-abraded substrates are reportedly not a prerequisite for deposition with some high growth rate techniques[14, 15, 118, 119] or with electron bombardment during filament-assisted

CVD.[120] Completely different nucleation routes must be invoked to account for diamond growth in these instances. Nucleation from caged carbon compounds[121] may explain some instances of gas-phase nucleation, but is an unimportant mechanism in ion-beam deposition or in CVD environments that have negligible concentrations of large hydrocarbons.

3.3 Diamond Growth on Nondiamond Substrates

The formation of continuous diamond films on nondiamond substrates proceeds by nucleation and three-dimensional growth of individual crystallites, followed by growth and eventual coalescence of the diamond particles into a polycrystalline film.[6, 18, 20] The general crystallite shape depends upon the growth conditions. Cubo-octahedra are produced at low carbon deposition rates, whereas more spherical and amorphous material results from higher carbon ratios. The transition of crystallite shape from cubic through various cubo-octahedra to octrahedra is determined by relative growth rates for (111) and (100) faces [v(111) and v(100), respectively.[122, 123] For example, octahedra would be produced with a growth rate ratio v(111)/v(100) of 0.58, whereas a ratio of 1.73 would yield cubic crystals.[122, 123] A larger degree of two-dimensional growth results in polyhedra truncated at the substrate surface, which gives a measure of diamond/substrate interfacial energy.[94]

For many applications, the morphologic and crystalline nature of the deposited diamond film are particularly interesting. The mechanical properties of the films are expected to depend on the crystalline texture and grain structure. Adhesion, wear behavior, and other interfacial characteristics may be affected by the surface structure. Control of surface morphology may be important for obtaining optically smooth surfaces, as polishing rates are orientation-dependent.

Kobashi and coworkers[122, 124] found that the dominant morphology of polycrystalline diamond films on Si, deposited by microwave-assisted plasma CVD, depends sensitively on carbon concentration: Triangular (111) facets are observed with $CH_4/H_2 < 0.4\%$; square (100) facets are dominant, with $0.5\% < CH_4/H_2 < 1.2\%$; microcrystallites with no clear faceting are found for CH_4/H_2 ratios above 1.5%. From stop-growth experiments, continuous cycles of renucleation were also observed.[122, 124] X-ray diffraction (XRD) data showed that the films are randomly oriented at low CH_4/H_2 ratios, with a slight (110)-preferred orientation from growth at high concentration.[122, 124] Other studies found that dominance of a particular diamond crystal facet is also a function of substrate temperature[125-128] and gas flow rate.[129]

Because of the differences in surface vacancy structures, the deposition rate for the various diamond planes is expected to be sensitive to the nature of the carbon transport species. Deposition of a single-carbon species may be preferred on (100) faces,[18] whereas insertion of a two-carbon molecule is calculated to be favorable to propagate growth on (111) planes.[130, 131] The concentration dependence of dominant film morphologies[122, 124] is also consistent with the mechanistic considerations. At low CH_4/H_2 concentrations, in which single-carbon gas-phase species may dominate, (100) growth is rapid and slower-growing (111) facets are observed; at higher concentrations, which favor formation of multicarbon molecules, (111) growth is preferred and (100) facets dominate.

The use of an intermediate layer of microcrystalline diamond (MCD) on Si[132, 133] results in films with different morphology from the case of bare Si substrates.[122, 124] Pyramidal features were observed for $CH_4/H_2 < 0.8\%$, and square (100) facets appeared in the range $1.0\% < H_4/H_2 < 1.2\%$. A rough, granular deposit appears between the facets. Most significantly, XRD analysis shows that the films deposited on MCD have a strong, (110)-preferred orientation,[129, 132-134] and an increase in nucleation density (~10x) was also reported. Diamond films with (111)-orientation have been prepared by using attached diamond seed particles[135] or low-flow rate deposition on Si substrates.[124] Deposition of crystals with (100)-orientation have also been reported,[136] but reproduction of this work has been difficult (D.C. Jeng 1990, private communication).

Wild et al[138, 139] have explored possible routes to (110)-preferred orientation. By using XRD measurements on successively thinned samples, they observed the evolution with thickness of a (110)-preferred crystalline texture for diamond films grown with combined microwave-filament activation.[138] The increase of a preferred orientation with increasing thickness can be successfully modeled by evolutionary selection: As individual crystallites grow and coalesce into a film, those with fast-growing tips or edges dominate while other are overgrown because of the anisotropic growth velocities.[139] It is possible for other textures (110) to develop under different growth conditions than those used in the aforementioned study:[139] For example, a (17, 3, 0) fiber texture was observed for specific conditions of filament-assisted diamond deposition.[127]

Although postgrowth sample analysis has significantly added to our knowledge base, there is little in situ work that could yield definitive answers concerning diamond crystal growth. Understanding the process of diamond nucleation is of paramount importance to technologic deployment, but remains a challenge for investigators.

4. Diamond CVD Gas-Phase Analysis

Characterization of the gas-phase in diamond CVD systems has focused on identification of the diamond "growth species" - the specific gas-phase atoms or molecules, such as atomic C, CH_3, or C_2H_2 – responsible for carbon transport to the deposition surface. Other important reactive species, such

as atomic hydrogen or OH, must also be monitored. In situ diagnostics have made a significant impact upon not only species detection, but also temperature determination.

4.1 Filament-Assisted CVD

Infrared diode laser absorption spectroscopy was the first method employed for in situ diagnostics of the filament-assisted diamond CVD growth process.[140-142] High concentrations of CH_4 and C_2H_2, as well as lower densities of CH_3 and C_2H_4, were detected during diamond growth from CH_4/H_2 mixtures. The probing laser beam sampled the region above the growth surface, but the measured concentrations were averages over the inhomogeneous gaseous regions. The measured C_2H_2 rotational temperature of ~600 K reflected an average gas-phase temperature from regions near the 2300 K filament and the cold chamber walls.

Conversion of a significant fraction of CH_4 to C_2H_2 is expected in the case of equilibration of the gas mixture at high temperature (Figure 5). Although the rapid diffusion of atomic hydrogen relative to the heavier hydrocarbons insures a nonequilibrium distribution of gas-phase species at the growth surface, calculation of gas-phase concentrations based on the assumption of thermodynamic equilibrium (EQ) agrees qualitatively with the observed densities.[140-142] The hydrocarbons CH_4, C_2H_2, CH_3, and C_2H_4 are all present in sufficient quantities to account for the diamond deposition individually. Although not detected, the densities of CH, CH_2, and C_3 predicted from an EQ model are too low for consideration as growth species.

Figure 5.

Calculated concentrations of gas-phase species for a 0.5% CH_4/H_2 mixture at thermal equilibrium. The H_2 curve is at a mole fraction of ~1, and is not shown, (From Ref. 141.)

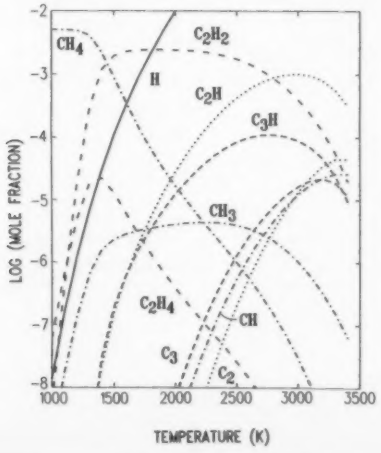

Harris and coworkers[106, 143, 144] have used mass spectrometry to detect stable species at the diamond deposition surface. By using a quartz sampling probe, whose tip was flush with Si[143] or Pt[106] substrates, or with the tip itself as the growth surface,[144] they find CH_4 and C_2H_2 as the major species, while C_2H_4 and C_2H_6 are minor constituents. Information about such radicals as CH_3 and H, which are expected to recombine in the sampling probe before reaching the mass spectrometer, was extracted from a kinetic analysis in combination with the determined CH_4, C_2H_4, and C_2H_6 concentrations (see Section 5.2.)[144] The analysis also shows the nonequilibrium composition of gaseous species in the mixture (Figure 6). The concentrations of CH_4, C_2H_2, CH_3, and C_2H_4 that were measured or calculated in this study were each sufficient to account for the diamond deposition. Larger hydrocarbons, with three to ten carbon atoms, occur in only trace quantities (quantified after being condensed and concentrated) and are unimportant for diamond growth.[106] Another sampling study, which employed a gas chromatograph detector,[145, 146] likewise identified CH_4, C_2H_2, C_2H_4, and C_2H_6 as the major species produced in a hot-filament diamond CVD reactor. Because of the similarity of gas-phase products that result from activation of CH_4/H_2 and C_2H_2/H_2 mixtures, thermodynamic equilibrium is a good approximation near the filament.

Isotopic labeling studies have been used with in situ sampling to yield strong evidence that the CH_3 radical is the primary diamond growth species under some conditions of CH_4/H_2 filament-assisted CVD.[147, 148] Mixed $^{12}C/^{13}C$ diamond films were deposited from nonequilibrated isotopic gas-phase mixtures of CH_4/H_2 or $CH_4/C_2H_2/H_2$. The isotopic content of the films was determined from the shift of the first-order diamond Raman band, while the major gas-phase constituents (CH_4 and C_2H_2) were sampled and analyzed by using matrix-isolation IR absorption spectroscopy. The measured isotopic fraction of the diamond films was similar to the estimated gas-phase CH_3 radical isotopic ratio and significantly different from the measured C_2H_2 ratio.

Two important radical species, H[142, 149-151] and CH_3,[142, 149, 152] were detected in situ during filament-assisted growth by using resonance-enhanced multiphoton ionization (REMPI) spectroscopy. Although a focused laser beam can lead to nondiscriminant photoionization of many species, REMPI schemes are used to detect H atoms selectively by using 365.5 radiation[150] and CH_3 radicals with 333.5 nm excitation.[152] The focused laser beam yields good spatial resolution, but it is necessary to insert a (possibly intrusive) electrode for photoelectron collection.

The variation of H atom concentration, [H], with filament temperature was determined at various CH_4/H_2 ratios (Figure 7).[150] The atomic hydrogen density monotonically increases, with a dependence that is largely in agreement with that expected from thermal dissociation of hydrogen. A slower increase is found at filament temperatures above 2500 K.[141] The quantity of atomic hydrogen decreases with the addition of CH_4. At the

higher methane/hydrogen flow ratios (e.g. 3% CH_4/H_2), a hysteresis in [H] vs. temperature is observed, which has been explained by carbon deposition on the filament surface.[153] The REMPI measurements above and below the filament are consistent with rapid diffusive transport of atomic hydrogen. REMPI studies of CH_3[142, 149, 152] shows that an increase in the initial CH_4 ratio (from 0.2 to 4.0%) or filament temperature (up to ~2600 K) results in increased CH_3 concentration. The concentration of another potential growth species, C_2H_2, also increases with CH_4/H_2 ratio, although at perhaps a faster rate.[142, 152] The dependence of the CH_3, signal on radial distance from the filament was also reported,[152] but has yet to be successfully modeled.

The REMPI results[150] suggest a significant surface role played by atomic hydrogen in diamond CVD. An increased CH_4/H_2 ratio produces the expected increase in both CH_3 radical and C_2H_2 concentrations, but a decrease in the H atom concentration. The quality of the deposited diamond, as judged by the Raman spectra, decreases as the CH_4/H_2 ratio is increased. It is thus concluded that filament-assisted diamond growth was not limited by production of CH_3 from H atom-driven reactions, but by surface reactions involving atomic hydrogen. Two possible surface reactions are H atom abstraction to produce a reactive site and etching of graphitic carbon by atomic hydrogen.[150]

The addition of oxygen-containing compounds enhances the filament-assisted diamond quality and growth rate.[154-156] A decrease in the C_2H_2/CH_4 ratio concomitant with O_2 addition is interpreted to indicate the role of C_2H_2 in amorphous or graphitic carbon deposition.[157] The major reaction products from oxygen addition are CO and H_2O, as detected with mass spectrometry.[158, 159] Thus, although oxygen decreases the effective carbon concentration by production of unreactive CO, it may also increase the CH_3/C_2H_2 ratio, as well as produce a small quantity of OH, which is an effective graphite etchant.[158]

Other detection techniques have been employed to monitor H atom concentration. Third-harmonic generation (THG) was used in a filament-assisted diamond CVD reactor.[142, 151] Although a promising technique for use in media that transmit vacuum ultraviolet radiation, THG detection of radicals is relatively new and more work is needed to correlate signal intensities with species concentration. The laser-excited fluorescence (LEF) method was recently used to measure absolute atomic hydrogen concentrations in H_2 and CH_4/H_2 mixtures near heated filaments.[160, 161] Radial concentration profiles from the filament were obtained, and the effect of various filament materials and diameters was explored. Measurements regarding the effect of CH_4 addition were complicated by carbon absorption by the filament, which in turn affected the temperature. There was, however, good agreement in absolute H atom concentrations determined with LEF measurements and mass spectrometric analysis.[144] The production of atomic hydrogen has also been deduced from the voltage-current characteristics of refractory filaments.[162] The simple detection technique could be useful for screening filament material, but can only be applied in nonreactive gas mixtures. Jansen et al[162] determined that nonequilibrium atomic hydrogen concentrations are produced from thin wires commonly used in filament-assisted diamond CVD reactors. Discrepancies with the LEF study[160,161] suggest that atomic hydrogen production may be quite system-dependent.

Gas-phase rotational temperatures have been measured with the coherent anti-Stokes Raman spectroscopy (CARS).[163, 164] Although the sensitivity limits of CARS restrict species detection to such reactants as H_2 and CH_4 or major products (e.g. C_2H_2), gas-phase density profiles and temperature measurements can be made in situ and are crucial inputs for gas-phase modeling.

4.2 Low Pressure Plasmas

Unlike the filament CVD systems, plasmas offer a ready source of self-diagnostic information in the form of visible light emission. Active species in the plasma can be identified by emission signatures, which could potentially be used as the basis for process control. For example, H, C, CH, OH, and CO emission can be identified in microwave discharges of CH_4/rare gas,[165] CH_4/H_2,[165, 167] and $CH_4/H_2/H_2O$[168] in which diamond deposition occurs. Unfortunately, only a limited number of species have excited states that emit detectable fluorescence. The importance of CH_3, C_2H_2, and C_2H_4, to

Figure 6.

Calculated time history of gas composition for a 0.3% CH_4/H_2 mixture at 2000 K. The symbols are: □, H; Δ, C_2H_2; ○, CH_4; ▽, CH_3; ■, C_2H_4; ●, CH_2; +, C_3H_3; x, C_4H_2. Using this model, the time to reach equilibrium is 5-10 s. (From Ref. 143, with permission.

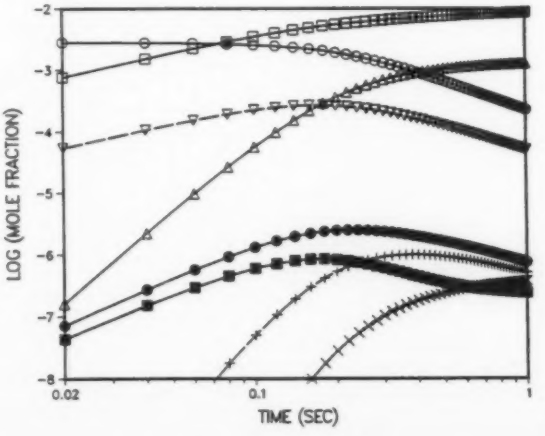

Figure 7.

Detection of atomic hydrogen in a filament-assisted diamond reactor using REMPI.CH_4 addition attenuates the H signal. Carbon deposition on the filament occurs with 3% CH_4/H_2 and severly decreases H atom production. (From Ref. 150, with permission.

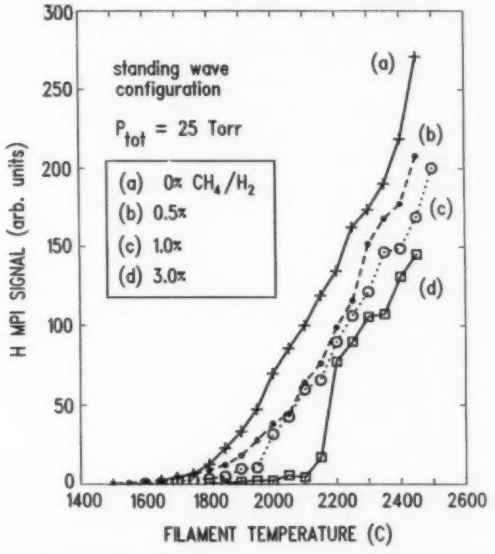

name but a few, cannot be directly assessed by using optical emission spectroscopy. Furthermore, the emission intensity is not simply related to the total concentration of the emitting species, even in a relative sense (see below). In general, many caveats regarding emission spectroscopy must be understood before mechanistic information can be extracted.

The determination of relative changes in species concentration from emission intensities is complicated because of the various processes that can affect the intensities. For instance, variation in plasma power may change the electron energy distribution and, consequently, the rate for excited-state production, thus leaving the ground-state density essentially constant. In this case, the resultant change in excited-state emission intensity would not reflect a change in ground-state population, which is typically ~10^6 higher concentration than the excited-state population.[169] To correct for such variation, the technique of actinometry is often employed. With actinometry the emission intensity of an inert species (the "actinometer") that has a similar excitation energy to the species of interest is monitored.[17] The intensity of the actinometer is used to normalize emission intensities and, thus, account for variations in the electron energy distribution or energy transfer pathways. In this way, information about ground-state concentrations can in some cases be inferred.[170]

Mucha et al[171] conducted an optical emission study of a microwave plasma tube reactor. By using actinometry with the hydrogen Balmer-α line, they deduced the effect of CH_4 and O_2 addition on ground state atomic hydrogen concentration (Figure 8). The H atom concentration, along with the diamond quality, decreases with increased CH_4/H_2 ratio and increases with added O_2. They presented evidence that O_2 passivates the quartz walls toward H atom recombination.[171] Other observed radicals (CH, C_2) have low excitation energy thresholds, for which actinometers are not available and reliable estimates of changes in ground-state concentrations cannot be made.

Inspektor and coworkers[172-174] have used optical emission to examine several microwave plasma diamond deposition chemistries. The deposition rates and emission intensities of CH, C_2, and atomic hydrogen were monitored in CH_4/H_2,[172] CH_4/rare gas/CH_2,[174] and various C/H/O[173] plasmas. In agreement with previous work,[171] oxygen addition increased the H atom emission intensity and improved the diamond film quality[173], even though surface effects were much less important in this study because of the larger reactor used.[173] The hydrogen emission intensity and diamond deposition rate both exhibited maxima, albeit at different CH_4/H_2 values (~1% and ~3%, respectively). However, because the emission intensities were normalized to those of pure hydrogen plasmas and not to rare gas emission lines [typically of low intensity in such reactors,[174]] definitive statements about concentrations could not be made.

Emission spectroscopy was also used in a study of CO/H_2/He plasmas.[175,176] Diamond deposition occurred with high H_2 concentration, when emission signals from C_2 and especially C were strongly attenuated. Some intensity decrease is due to changes in the electron energy distribution; this was determined when actinometry of the hydrogen Balmer-α xline was used. Although some of the conclusions in this work[175,176] cannot be substantiated by the presented data, conditions that produce stronger C_2 and C emission tend to correlate with deposition of non-diamond carbon in many discharge systems.

A $CO/CO_2/H_2$ microwave diamond deposition system was recently explored by using optical emission, exhaust gas analysis, and the study of alternating deposition and etching reactions.[177] Emission bands of both CO and OH were detected in CO_2/H_2 mixtures, but only CO bands were seen in CO/H_2 plasmas. The exhaust gas composition for CO/H_2 plasmas was lower in CO and higher in CH_4 and C_2H_2 than corresponding carbon fractions of CO_2/H_2 mixtures. The carbon etch rate increased in the order $CO<CO_2<O_2$. Deposition was suppressed when O_2 (or CO_2) was added to the CO/H_2 plasma when compared with successive CO/H_2 and O_2/H_2 deposition and etching cycles. This study indicates that oxygen-containing gases alter the deposition chemistry, and perhaps also provide enhanced etching of nondiamond carbon deposits. The generality of the work remains to be seen, as results can be quite reactor-dependent.

For both kinetic and flow modeling, the gas kinetic temperature is an important parameter to determine. In low pressure (<1 mbar) plasmas, the electron temperature may be quite high (~10eV>10^5 K), whereas the gas kinetic temperature is only slightly about ambient temperature.[169] As the electron mean-free-path decreases at higher pressure, the difference between the gas and electron temperatures decreases. Although there is some temperature information on filament diamond CVD reactors,[144, 163] the gas temperature in plasma reactors is not typically known. The gas kinetic temperature in a 40 mbar dc discharge diamond CVD reactor has recently been measured by using rotationally-resolved emission spectroscopy[178, 179] and confirmed by using LEF.[179] The intensities of individual rovibronic emission lines from either H_2 or CN (impurity) indicate gas temperatures in the 1200-1300 K range, slightly higher than that of the deposition surface. Using CARS, Roman et al[164] reported H_2 rotational temperatures of 300-400 K in a 13 mbar rf plasma. Although the gas temperature is expected to be lower at reduced pressures, the large difference between the temperature determinations must also be caused by details of the power density and energy transfer mechanisms in the two plasmas. Temperature characterization of diamond-depositing plasmas for a range of pressures needs to be performed by using these and other diagnostic methods.

There has been comparatively little work in the direct detection of ground-state species in diamond CVD microwave or dc plasmas. Ground-state atomic hydrogen was detected in a dc plasma system by THG.[180, 181] Although the spatially-resolved emission from excited-state atomic hydrogen is strongly peaked in discrete regions,[181] the distribution of ground state H atoms is considered relatively uniform because of rapid diffusion.[180] The low atomic hydrogen density measured is consistent with the low diamond growth rate, which is typically obtained with the dc discharge method.

Mass spectrometry yields important information on ground-state species in plasma environments, because it can detect ionic, as well as radical or stable, neutral species. Preliminary accounts have recently been reported on application of mass spectrometry to diamond deposition plasmas.[182, 183] In microwave[182] and dc[183] plasmas, CH_3 was detected by using low-energy electron impact ionization[184, 185] to discriminate against dissociative ionization of CH_4. The diamond growth rate shows a dependence on CH_4/H_2 ratio, which is similar to that of the CH_3 signal dependence.[183]

Figure 8.

Relative atomic hydrogen concentrations in a microwave diamond CVD reactor from optical emission. The intensity of the 656 mn line of H atom is ratioed to that of the Ar 750 nm line. Addition of CH_4 decreases the H atom density, while O_2 addition causes a large increase. (From Ref. 171, with permission.)

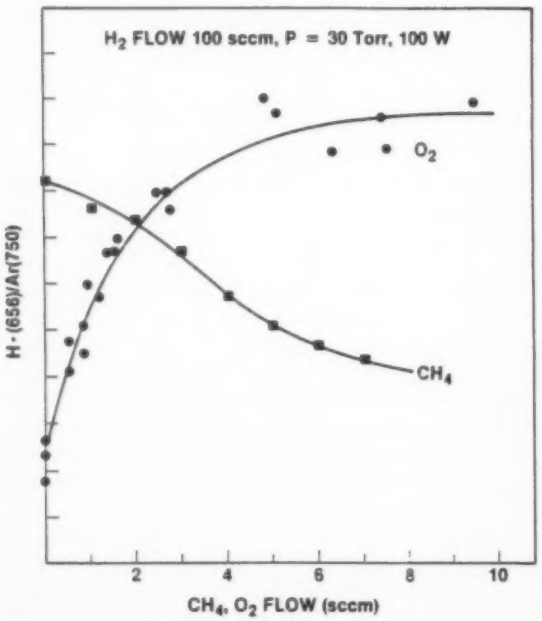

4.3 Plasma Torches

As with low-pressure plasmas, optical emission has been utilized for initial characterization of higher pressure dc plasma torches.[186-190] Atomic hydrogen, CH, and C_2 emission is detected from CH_4/H_2 mixtures, but emission from excited-state H_2, commonly seen in microwave plasmas, is absent, which suggests near-complete dissociation of H_2 in the arc jet.[186] Without the cooled substrate present, the gas temperature as measured with a thermocouple is 2000-2500° C.[186] A much higher value of ~5000 K, which was derived from the relative intensities of the H atom emission lines, led to the suggestion that atomic carbon was the diamond growth species.[187, 188]

The temperature determinations in a diamond-depositing dc arc jet190 provide a clear and instructive example of one drawback of optical emission analysis. Excited electronic species of C2 and CH were detected in emission, whereas ground-state CH was monitored by using LEF (Figure 9). Temperature measurements of the arc jet were in apparent disagreement, with a value of ~5000 K extracted from the C2 emission intensity and 2100 ± 100 K as determined from the CH radical LEF spectrum. Because the LEF measurements are made on the ground-state CH species, the observed value of 2100 K was believed closer to the true gas kinetic temperature. The 5000 K determination was not thought to represent a "temperature" (in the sense of an equilibrated state of gas molecules); rather, the emission intensity distribution was due to the nonthermal distribution of rovibronic states populated upon excitation. In the case of C_2, excitation evidently occurs through chemiluminescent reactions, even be-

yond the plasma zone, and the resultant emission reflects the nascent product distribution before relaxation and equilibration by gas phase collisions. By analogy, measurements of temperature based on atomic hydrogen emission intensities[188, 189] are indicative of the electron excitation process and not the gas-phase temperature. This is an important distinction, as gas-phase kinetics, which play a major role in determining radical concentrations, depend upon the gas kinetic temperature. Also, the presence of the deposition substrate, e.g. removed during optical probing of the arc jet,[190] may alter the gas-phase temperature and/or radical concentrations present under diamond growth conditions.

Mitsuda et al[191] have reported differences between excited-state concentrations derived from optical emission and measured ground-state species concentrations by using in situ mass spectrometry in a microwave plasma jet.[191] Strong C and nonthermal C_2 emission was observed from $Ar/H_2/CH_4$ and $Ar/H_2/C_2H_2$ plasma jets (although little H* emission!), whereas abundant CH_4 and C_2H_2 signals were observed by using mass spectrometry with sampling through the substrate. Higher hydrocarbons (e.g. C_3H) were also detected. Although the emission data suggest that C and C_2 are major species in the plasma, their concentrations at the growth surface are low and not considered important for diamond deposition.[191] Reactions occurring at the surface boundary layer (~1 cm thickness) were proposed to account for the diagnostic observations, but this may be another instance in which the optical emission spectrum does not reflect the plasma chemistry. This work[191] also provides a clear example of the need for in situ measurements while the deposition substrate is present.

Figure 9.

Characterization of a diamond-depositing dc arc jet: (a) C_2 chemiluminescence spectrum and simulated spectra. The best fit was ~5000 K. (b) Boltzmann plot of CH line intensities, obtained by LEF, which indicates a rotational temperature of 2140 K. (From Ref. 190, with permission).

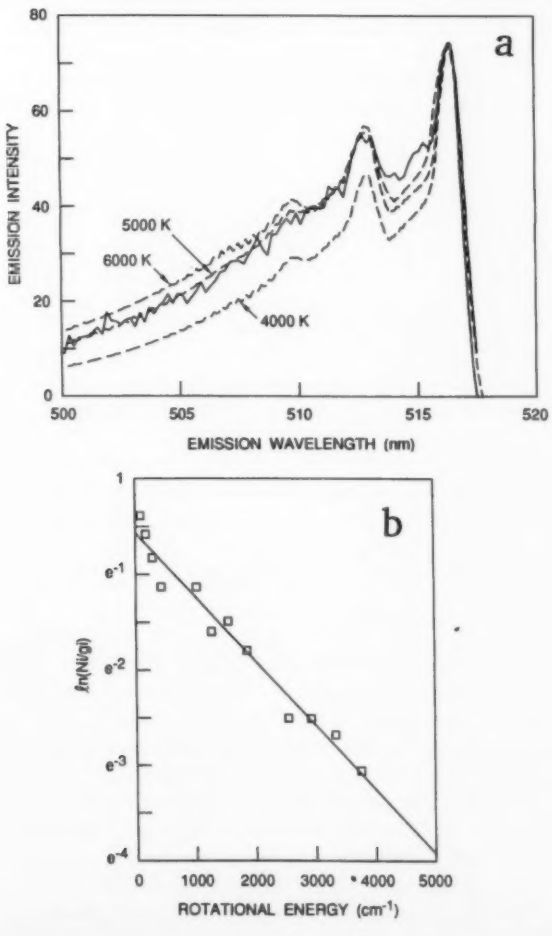

4.4 Combustion Flames

The demonstration of high-rate diamond growth in combustion flames has brought together the somewhat disparate realms of combustion chemistry and CVD. Using optical emission, Hirose et al[192] described conditions for production of optically transparent diamond crystals by using an oxy-acetylene combustion flame torch. Both LEF and sampling mass spectrometry were used in further mechanistic studies.[193] Spatial and parametric variation of C_2 and OH concentrations were obtained with LEF and indicate equilibrium concentrations. By correlation with the deposition rate, CH, C_2,[193] or CH_3[194] were considered candidates for growth species, whereas C_2H_2 was eliminated (Figure 10).

Planar laser-induced fluorescence and optical emission imaging has been reported for a diamond-depositing oxy-acetylene torch.[195] The observed steady-state flame emission from CH was interpreted as chemiluminescence, which resulted from reaction between C_2 and OH radicals:

$$C_2 + OH \rightarrow CH^* (A^2\Delta) \rightarrow CH (X^2\Pi) + h\nu\,(431\text{nm})$$

Emission from the excited CH ($A^2\Delta$) state was also stimulated by pulsed laser excitation at 193 nm. The laser-excited emission was thought to be due to absorption by and dissociation of C_2H radicals to produce C_2, which then reacts with OH by the above route. However, because other pathways could also generate CH* [for example, $CH_3 + h\nu(193\text{ nm}) \rightarrow CH^* + H_2$][196], confirmation of the C_2H assignment is needed.

The imaging technique of Fourier transform infrared tomography has been employed to characterize the spatial variation of gas-phase species in an oxy-acetylene flame

deposition system.[197,198] The characteristic signature IR spectra of CO, CO_2, and H_2O were identified, and relative concentration profiles were obtained. Measured gas temperatures of ~4200 K are higher than the predicted value of ~3300 K.[198] The temperature and species concentrations are perturbed by the presence of the deposition surface, which again highlights the need for true in situ measurements. Infrared tomography is a general and nonintrusive method that would be useful for probing other plasma environments.

4.5 Kinetic Studies

Several experiments have provided mechanistic information on diamond CVD growth without specific identification of gas-phase species. Typically, the diamond deposition rate was the observable monitored as deposition conditions were varied. The results have been interpreted in terms of heterogeneous reactions at the growth surface.

Angus and coworkers[199] were the first to make kinetic measurements on a thermally-activated diamond CVD reactor. The carbon deposition rate is first-order with respect to methane concentration, but half-order with ethylene concentration.[199] These results are consistent with a diamond growth species (either in the gas-phase or adsorbed on the surface), which contains a single carbon atom. Also, the presence of excess hydrogen increased the diamond yield by decreasing the graphite deposition rate. As the growth surface eventually becomes covered with graphite, alternating cycles of deposition and etching with hydrogen are needed to sustain diamond growth.

Figure 10.

Measured diamond growth rates for various C_2H_2/O_2 ratios in an oxy-acetylene combustion flame are shown in comparison with growth rates calculated by assuming a particular growth species (lines, as indicated). (From Ref. 194 with permission).

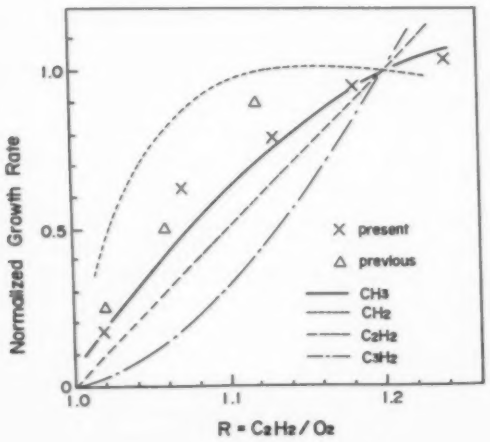

Atomic hydrogen may play numerous roles in the diamond CVD process, as summarized by Anthony.[200, 200a] In addition to those already discussed (i.e. stabilization of diamond surfaces, generation of hydrocarbon radicals, etching of graphite), atomic hydrogen also generates vacant surface sites and provides a minimum in carbon solubility as a function of gas temperature. Derjaguin & Fedoseev[16] originally discovered that higher diamond growth rate could be achieved by dissociation of H_2 to yield a supersaturation of atomic hydrogen. Heterogeneous reactions involving H atoms, such as preferential etching of graphitic carbon and preparation of vacant surface sites, were thought to be responsible for the enhanced growth rates, but gas-phase reactions that might lead to homogenous nucleation were also considered.[16]

An isotopic substitution experiment by Vakil et al[201] indicates that the breaking of a C-H bond is involved in the rate-limiting step of diamond growth. The diamond growth rate in a filament-assisted reactor was measured in situ with either CH_4/H_2 or CD_4/D_2 mixtures, and under the condition of constant filament power. The CD_4/D_2 deposition rate was lower than that of the CH_4/H_2 rate by a factor of $\sqrt{2}$. This result is precisely that expected for the case of a primary isotope effect, in which hydrogen is involved in the rate-controlling step.

To simplify and understand the gas-phase chemistry leading to growth. Martin & Hill[202, 203] demonstrated diamond deposition in a 4 mbar microwave-discharge flow system. Atomic hydrogen was produced in a remote Ar/H_2 discharge and reacted with CH_4[202, 203] or C_2H_2[203] at the entrance of a constant temperature (1100 K) furnace. Diamond crystals were deposited in both cases, but with higher quality and at a higher rate in the case of CH_4 injection. Although no in situ concentrations were measured, consideration of dehydrogenation kinetics leads to the conclusion that CH_3 is the primary growth species,[202] and reacts much more rapidly than C_2H_2 to deposit diamond.[203] However, because of the use of diamond-abraded silicon substrates, the nucleation and growth steps were not deconvoluted in this study.

4.6 Novel Systems

Most of the diamond CVD literature deals with C/H chemistry, with some emphasis on improvements due to perturbation with oxygen addition. The recent demonstration[204] of diamond deposition at low substrate temperatures (~550 K) by thermal activation of CH_4/F_2 or halocarbon/H_2 mixtures is a significant breakthrough and may involve substantially different chemistries and mechanisms than those occurring in the C/H system. Diamond growth from thermally activated CF_4/F_2 mixtures was also claimed,[205] but the etching of hydrocarbons off of the chamber walls may have played a key role in those experiments.

Figure 11.

Phase diagram for the C/H system predicted from the QET model, with the substrate temperature T plotted vs. the carbon fraction, γ_c. The diamond (d) and graphitic (g) boundaries at 36 Torr and the diamond boundary at 760 Torr [d(760)], are shown. Conditions of observed diamond (□, ○) and graphitic carbon (•) deposition are included. (From Ref. 208, with permission.)

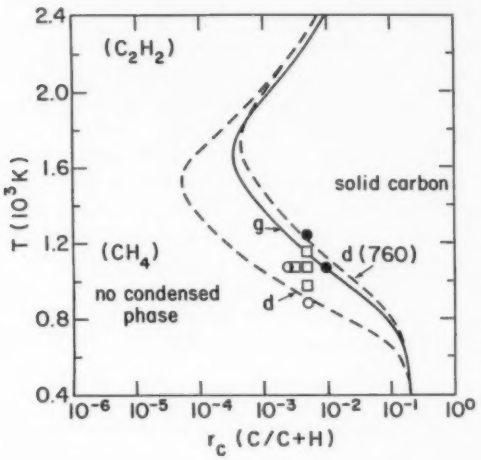

5. Gas-Phase and Surface Modeling

Computational modeling has considerably enhanced our understanding of the diamond CVD process. Although only a few species in a complex mixture can typically be detected in a given experiment, models of the reaction mechanism can be verified by comparison with in situ measurements and provide predictions for nondetected species. In addition, numerical calculations of surface reactions and surface-adsorbate energetics provide plausible schemes to describe diamond growth on the molecular level.

5.1 Equilibrium Models

Several workers[141, 164, 206, 207] have presented the results of EQ calculations for the gas-phase in filament-assisted diamond growth (Figure 5). The EQ approach is suitable for estimating the species prepared by considering the filament as purely a thermal source. Stable species at ~2000° C included C_2H_2, C_2H, and CH_3. The concentrations of C_2, CH, and C_3, species often detected in plasma emission, were calculated to be negligible.

Smith and coworkers[153, 208, 209] have presented a quasi-equilibrium theory (QET) model for diamond CVD. Using the equilibrium model as a basis, a term was added that represented enhanced etching of graphite over diamond. With inclusion of the nonthermodynamic etching term, conditions for which diamond deposition occurs have been identified over a range of pressures (Figure 11). The QET model has been successful in accounting for diamond deposition over a range of pressure conditions. Also, the QET prediction of carbon deposition on filaments explains some experimental observations of gas-phase species concentrations.[153] An EQ model has also been used to account for the observed conditions of carbon deposition in combustion flames.[210] The preponderance of nonthermal species generation discounts effective usage of an EQ model for plasma deposition environments.

5.2 Kinetic Models

Although an EQ model may predict the gas-phase distribution initially prepared by a filament, the flux of species incident on the diamond growth surface depends upon species transport and subsequent gas-phase reaction in the cooler region between filament and substrate. The diffusion velocity of atomic hydrogen, a principal gas-phase component, is much faster than heavier carbon-containing molecules and leads to a higher density of H atoms in cooler regions far-removed from the filament zone than predicted by EQ considerations. The resultant supersaturation of atomic hydrogen can also create nonequilibrium concentrations of radicals through gas-phase or surface reactions. Thus, the EQ model must be modified or supplanted by kinetic models to predict gas-phase concentrations near the growth surface accurately.

Harris et al[143] provided the first computational analysis of filament-assisted diamond growth. A zero-dimensional kinetic reaction model, which assumed a fixed temperature profile, was applied. The reaction rate data were based upon the considerable hydrocarbon combustion literature. The authors concluded that only CH_3, C_2H_2, CH_4, and C_2H_4 should be considered viable growth species, with the former two favored on the grounds of chemical reactivity. Similar kinetic analysis was used to model measured CO concentrations in the $CH_4/O_2/H_2$ system successfully.[158] In other analyses, the absolute concentrations of CH_3 and H atoms were extracted from mass spectrometric measurements of stable species, as the CH_3 generation reaction,

$$CH_4 + H \rightarrow CH_3 + H_2$$

is in partial equilibrium, and the primary source of C_2H_4 and C_2H_6 is CH_3 radical recombination.[144]

A similar kinetic model has been analyzed by Frenklach,[211] who found that the effect of H_2 was to suppress formation of aromatics, which promote nondiamond carbon deposition. A complete diamond growth model, which includes estimation of reaction rates at the diamond (111) surface, was recently presented.[212] Diamond growth by the irreversible addition of C_2H_2 was two to four orders of mag-

nitude faster than other growth pathways, such as CH_3 addition, in contradiction to the experimental findings of Martin & Hill[202,203] and Chu et al.[147,148] Many trends generally observed in filament-assisted diamond CVD systems, such as the dependence of deposition rate and diamond film quality on substrate temperature, were reproduced by the model. The important roles of atomic hydrogen were predicted to be the formation of diamond radical sites and the conversion of sp^2- to sp^3-bonded carbon. The conversion of graphitic and amorphous carbon by atomic hydrogen was also seen in simple statistical model of diamond growth.[213]

Matsui & Sahara[214] presented a kinetic model of a CH_3OH/H_2 hot-filament growth system, which showed that CH_3 is the only carbon-containing radical species of significance. The authors concluded that methyl radical was the diamond growth species assuming a reactive sticking coefficient of $\sim 10^{-2}$, although CO, CH_4, and C_2H_2 had higher calculated concentrations.

The proposal that stable carbon-containing molecules could lead to diamond growth was inferred from a kinetic model[215] of early, non-activated diamond growth experiments.[199] Diamond was deposited by passing a CH_4/H_2 mixture over diamond seed crystals held at 1420 K, with no plasma or high temperature activation. Because the gas residence time was too short for equilibration at the substrate temperature, there was little conversion of CH_4 into other active species. For instance, the calculate mole fraction of CH_3 was $\sim 10^{-6}$.[215] Harris[215] concluded that CH_4 was the diamond growth species in the nonactivated growth.[199]

Kinetic modeling[216] has been used to analyze the flow tube diamond CVD experiments of Martin & Hill.[202,203] Thermal diffusion and heterogeneous loss of H atoms were both included in the one-dimensional flow model. Methane and methyl radical are the only species predicted to have sufficient concentrations for the observed diamond deposition. Considering CH_3 as the growth species implies a reactivity of 10^{-3} to account for the growth rate. The reaction rate for C_2H_2 to form diamond is lower than 10^{-5}, with a propensity for deposition of nondiamond carbon.[216]

Kinetic analysis has also been applied to diamond-depositing oxy-acetylene combustion flames[193,194] and dc torches.[190] The CH_3 radical concentration, in equilibrium in the flame growth environment, correlates well with the diamond deposition rate.[194] The C atom concentration is in super-equilibrium at the growth surface in the dc torch, and was proposed as the growth species in that system.[190] Treatment of the gas flow and reactions at the boundary layer in the vicinity of cooled substrates is a difficult problem and may have a large effect on the active species impinging on the growth surface in these high flow rate systems.

Goodwin & Gavillet[217,218] have extended a kinetic model of the filament-assisted environment to include transport phenomena, by using a one-dimensional geometry and calculated flow field and temperature profile (Figure 12). The agreement between the calculated values and the available experimental data is good. Conclusions regarding possible growth species (CH_3, C_2H_2, and CH_4) are similar to the Harris analysis.[144] Consideration of surface recombination of atomic hydrogen also affected the predicted species profiles.[218] The availability of such detailed models demands that spatially resolved concentration and temperature profiles be determined.

5.3 Theoretical Growth Models

As a model of growth on the (111) diamond surface, Tsuda et al[219,220] considered carbon deposition from CH_3 and CH_3^+ species. Propagation of the crystal lattice occurs by monolayer addition of CH_3 groups. The minimum energy pathway for CH_3^+ induced bonding of adjacent methyl groups was determined by using semi-empirical molecular orbital calculations on model compounds of 9-13 carbon atoms. Although charged species may play important roles in some plasma environments, the Tsuda model is often discounted because of the presumed lack of ionic species in filament-assisted diamond CVD systems, which typically yield growth rates higher than in microwave or dc plasma systems.

Figure 12.

Gas-phase species concentrations calculated from a one-dimensional kinetic model for a filament-assisted CVD reactor and initial 0.3% CH_4/H_2 mixture. The H recombination at the growth surface was included in this model. (From Ref. 218, with permission.)

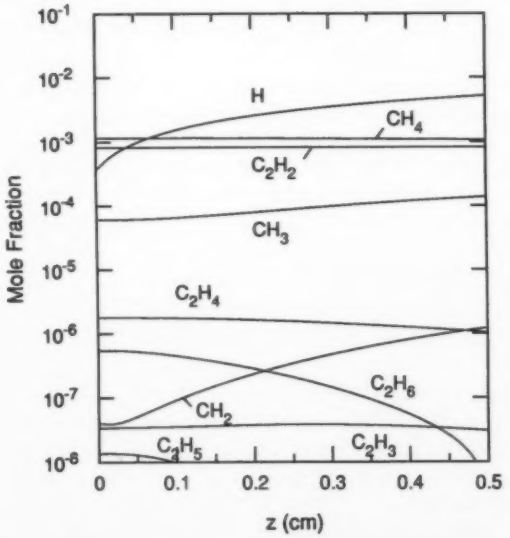

Considering the gas-phase species present at high temperature, Frenklach & Spear[130] proposed a diamond growth model based on carbon deposition by C_2H_2 addition. Reactive surface sites were prepared by hydrogen atom abstraction. The competing pathway of graphitic carbon deposition was also described by using C_2H_2 reactions. Molecular orbital calculations on a 9-carbon model compound verified that, following an activated hydrogen abstraction step, diamond lattice growth by C_2H_2 addition was energetically favorable.[131]

Harris[221] has proposed a diamond growth model based on CH_3 addition to the (100) surface. The model compound bicyclo-nonane (BCN), which consists of nine carbon atoms, is considered to represent the diamond lattice. Rate constants for the various reaction steps were determined either from analogous gas-phase kinetic measurements or Benson's rules for enthalpy and entropy changes in hydrocarbons.[222] [A recent ab initio study of bond relaxation in a (111) diamond model compound of four carbon atoms showed only a small energetic difference with the corresponding gas-phase transition state values, which justifies the use of bond energies and activation energies from gas-phase hydrocarbon reactions.[223]] Using gas-phase concentrations from in situ measurements, integration of the rate constants allowed the time history of an ensemble of BCN molecules to be followed.[221] The resultant diamond growth rate (0.06-0.6 μm/hr) closely resembles typically observed rates. The estimated cumulative error in the predicted growth rate was two orders of magnitude, but the calculations clearly demonstrate CH_3 addition as a feasible pathway for diamond growth.

Goodwin[224] has coupled the Harris CH_3 model[221] for diamond (100) surface growth with gas-phase simulations of oxy-acetylene flame[193] and dc torch[190] experiments. The model includes gas-phase kinetics and transport, as well as gas-surface kinetics. The calculated growth rates (20-120 μm/hr) are in excellent agreement with the experimental values. These results show that the assumption of CH_3 as the sole growth species can account for a wide range of observed diamond deposition rates.

The energetics and dynamics of radical-surface interactions at the diamond surface are now being addressed in several theoretical studies. Semi-empirical calculations were performed by using a $C_{20}H_{35}$ cluster for the diamond (111) surface.[69] No activation barrier for the hydrogen abstraction step was found, unlike the previous study.[131] Methyl radical addition gives rise to significant steric repulsion at high coverages. Because of the strong experimental evidence for CH_3 as growth species, the calculation suggests that the critical configuration involves two, not three, adjacent reactive sites.[69] Bond energies for CH_3, C_2H, and C_2H_2 to a $C_{13}H_{21}$ cluster have also been calculated.[225-227] A molecular dynamics simulation of atomic hydrogen reactions found that unsaturated carbon bonds were quickly saturated by hydrogen, and that the creation of short-lived radical sites occurred with little disruption of the carbon lattice.[228]

6. Summary

The diamond CVD process shows great promise for impacting a variety of technologic areas. Unfortunately, our understanding of diamond CVD mechanisms is far from complete. The CVD diamond interface with many substrates has been explored, but the nucleation process remains a mystery. Information on surface growth processes is mostly indirect, even though the structure and reactivity of diamond single crystal faces have been studied. The gas-phase composition in CVD reactors is reasonably well characterized for the case of filament-assisted deposition, whereas probing and modeling of plasma-assisted environments are more difficult and currently incomplete. Diamond CVD with oxy-acetylene flames seemingly presents a favorable case for mechanistic understanding, given the wealth of literature on combustion flame characterization and modeling. However, due to the complicating presence of the growth surface in the combustion flame (or other torches), our knowledge of the deposition chemistry is no better than for other diamond CVD techniques. A more detailed picture will presumably emerge as more effort is brought to bear on the high growth rate diamond deposition processes.

In the near future, the use of in situ probes may aid in optimization of various diamond CVD processes by providing for maximization of the flux of diamond precursors to the surface, while minimizing the competing deposition of other carbon forms. The coupling of ab initio calculations of surface structures and interactions with realistic models of gas-phase species densities and flow dynamics will lead to a more complete description of the diamond growth mechanism. Nonintrusive probes and chemical mechanisms used for analysis might then form the basis for future "smart" process monitoring and control schemes.

Acknowledgements

We acknowledge Pehr Pehrsson, John Russell, Helen Thorsheim, and Maureen Hanratty for a careful reading of the manuscript and many helpful comments. This work was supported in part by the Office of Naval Research, the Innovative Science and Technology Office of the Strategic Defense Initiative Organization, and the Air Force Office of Scientific Research.

Biographies

Dr. Francis Celli is a member of the Technical Staff in the Central Research Laboratories of Texas Instruments, Inc. While a National Research Council Postdoctoral Fellow at the

Naval Research Laboratory from 1987-89, he made some of the first in situ gas phase measurements of diamond CVD processes. At TI, Dr. Celii investigated the use of diamond in microelectronics packaging applications. He is currently applying real-time spectroscopic approaches for process monitoring and control of III-V materials growth techniques, such as molecular beam epitaxy.

Dr. James E. Butler is a Research Chemist and heads the Gas/Surface Dynamics Section of the Chemistry Division at the Naval Research Laboratory, Washington, DC. His research group studies the gaseous and surface chemical processes occurring in the chemical vapor deposition and etching of materials. Dr. Butler's research includes the in situ characterization of the gaseous and surface species, the development of models of the diamond deposition chemistry, the characterization of deposited materials, and the development of diagnostic techniques. Dr. Butler has coordinated the NRL accelerated research initiative on "Film Growth mechanisms: Diamond" since 1987 and serves as technical advisor and consultant for diverse diamond related programs of other government agencies including the Defense Advanced Research Projects Agency, Office of Naval Research, and the National Science Foundation.

References

1. Bruton, E. 1978. *Diamonds*, London: NAG
2. Field, J.E. 1979. *The Properties of Diamonds*, New York: Academic
3. Nassau, K., Nassau, J. 1979. J. Cryst, Growth 46: 157-72
4. Spitsyn, B.V., Derjaguin, D.B. 1975. *Sci. Am.* 233: 102-9
5. DeVries, R.C. 1987. *Annu. Rev. Mater. Sci.* 17: 161-87
6. Messier, R., Badzian, A.R., Badzian, T., Spear, K.E., Bachmann, P., Roy, R. 1987. *Thin Solid Films* 153: 1-9
7. Martin, J. 1990. *Ind. Diamond Rev.* 50: 291-93
8. Bachmann, P.K. 1990. *Adv. Mater.* 2: 195-99
9. Matsumoto, S., Sato, Y., Tsutsumi, M., Setaka, N. 1982. *J. Mater. Sci.* 17: 3106-12
10. Matsumoto, S., Sato, Y., Kamo, M., Setaka, N. 1982. *Jpn. J. Appl. Phys.* 21: L183-85
11. Kamo, M., Sato, Y., Matsumoto, S., Setaka, N. 1983. *J. Cryst. Growth* 62: 642-44
12. Pauling, L. 1960. *The Nature of the Chemical Bond*, p. 85. Ithaca: Cornell Univ. Press
13. Klocek, P., Hoggins, J., Taborek, P., McKenna T. 1990. *Proc. SPIE Conf. Diamond Opt. III* 1325: 63-72
14. Snail, K.A., Hanssen, L. 1991. *J. Cryst. Growth* 112:651-59
15. Geis, M.W., Efremow, N.N., Rathman, D.D. 1988. *J. Vac. Sci. Technol. A6*: 1953-54

15a. Collins, A.T. 1989. *Semicond. Sci. Technol.* 4:605-11

16. Badzian, A.R., DeVries, R.C. 1988. *Mater. Res. Bull.* 23: 385-400
17. Spitsyn, B.V., Bouilov, L.L., Derjaguin, B.V. 1988. *Prog. Cryst. Growth Charact.* 17:79-170
18. Angus, J.C., Hayman, C.C. 1988. *Science* 241: 913-21
19. Angus, J.C., Buck, F.A., Sunkara, M., Groth, T.F., Hayman, C.C., Gat, R. 1989. *MRS Bull.* 14: 38-47
20. Spear, K.E. 1989. *J. Am. Ceram. Soc.* 72:171-91
21. Bachmann, P.K., Messier, R. 1989. *Chem. Eng. News* May 15: 24-39
22. Yarbrough, W.A., Messier, R. 1990. *Science* 247: 688-96
23. Tsai, H.C., Bogy, D.B. 1987. *J. Vac. Sci. Technol.* A5: 3287-3312
24. Angus, J.C., Koidl, P., Domitz, S. 1986. *Plasma Deposited Thin Films*, ed. J. Mort, F. Jansen, Chap. 4, pp. 89-127, Boca Raton, Fla: CRC
25. Sappok, R., Boehm, H.P. 1968. *Carbon* 6: 283-95
26. Thomas, J.M., Evans, E.L. 1975. *Diamond Res.* 3: 2-8
27. Derry, T.E., Madiba, C.C.P., Sellschop, J.P.F. 1983. *Nucl. Instrum. Methods Phys. Res.* 218: 559-62
28. Hansen, J.O., Copperthwaite, R.G., Derry, T.E., Pratt, J.M. 1989. *J. Colloid Interface Sci.* 130: 347-58
29. Sappok, R., Boehm, H.P. 1968. *Carbon* 6: 573-88
30. Lander, J.J., Morrison, J. 1966. *Surf. Sci.* 4: 241-46
31. Matsumoto, S., Setaka, N. 1979. *Carbon* 17: 485-89
32. Matsumoto, S., Kanda, H., Sato, Y., Setaka, N. 1977. *Carbon* 15: 299-302
33. Abyzov, A.M., Smirnov, E.P. 1989. *Kinet. Catal.* 30: 796-802
34. Vleeschdrager, E. 1986. *Hardness 10: Diamond.* Paris: Gaston Lachurie
35. Yang, C., Tokura, H., Yoshikawa, M. 1988. *Polishing of Diamond Film with Metal*, Tokyo Inst. Technol. Intern. Rep. 152
36. Harker, A.B., Flintoff, J., DeNatale, J.F. 1990. *Proc. SPIE Conf. Diamond Opt. III* 1325: 222-29
37. Mason, F. 1990. *Am. Mach.* April: 49-52
38. Pate, B.B. 1986. *Surf. Sci.* 165: 83-142
39. Lurie, P.G., Wilson, J.M. 1977. *Surf. Sci.* 65: 476-98
40. Lurie, P.G., Wilson, J.M. 1977. *Surf. Sci* 65: 499-510
41. Farnsworth, H.E., Marsh, J.B., Toots, J. 1962. *Proc. Int. Conf. Semicond. Exeter*, pp. 836-41
42. Marsh, J.B., Farnsworth, H.E. 1964. *Surf. Sci.* 1: 3-21
43. Lurie, P.G., Wilson, J.M. 1977. *Surf. Sci.* 65: 453-75
44. Yang, W.S., Sokolov, J., Jona, F., Marcus, P.M. 1982. *Solid State Commun.* 41: 191-93

45. Sowa, E.C., Kubiak, G.D., Stulen, R.H., Van Hove, M.A. 1988. *J. Vac. Sci. Technol.* A6: 832-33

46. Hamza, A.V., Kubiak, G.D., Stulen, R.H. 1988. *Surf. Sci.* 206: L833-44

47. Vidali, G., Frankl, D.R. 1983. *Phys. Rev.* B27: 2480-87

48. Vidali, G., Cole, M.W., Weinberg, W.H., Steele, W.A. 1983. *Phys. Rev. Lett.* 51: 118-21

49. Pate, B.B., Stefan, P.M., Binns, C., Jupiter, P.J., Shek, M.L., et al. 1981. *J. Vac. Sci. Technol.* 19:349-54

50. Pepper, S.V. 1981. *Appl. Phys. Lett.* 33: 344-46

51. Pepper, S.V. 1982. *J. Vac. Sci. Technol.* 20: 643-46

52. Pate, B.B., Waclawski, B.J., Stefan, P.M., Binns, C., Ohta, T., et al. 1983. *Physica* 117B/118B: 783-85

53. Kubiak, G.D., Kolasinski, K.W. 1988. *J. Vac. Sci. Technol.* A6: 814-16

54. Namba, H., Masuda, M., Kuroda, H. 1988. *Appl. Surf. Sci.* 33/34: 187-92

55. Pate, B.B., Hecht, M.H., Binns, C., Lindau, I., Spicer, W.E. 1982. *J. Vac. Sci. Technol.* 21: 364-67

56. Waclawski, B.J., Pierce, D.T., Swanson, N., Celotta, R.J. 1982. *J. Vac. Sci. Technol.* 21: 368-70

57. Haneman, D. 1961. *Phys. Rev.* 121: 1093-1100

58. Pandey, K.C. 1981. *Phys. Rev. Lett.* 47: 1913-17

59. Pandey, K.C. 1982. *Phys Rev.* B25: 4338-41

60. Pandey, K.C. 1982. *Phys. Rev. Lett.* 49: 223-26

61. Chadi, D.J. 1982. *Phys. Rev.* B26: 4762-65

62. Northrup, J.E., Cohen, M.L. 1982. *Phys. Rev. Lett.* 49: 1349-52

63. Vanderbilt, D., Louie, S.G. 1984. *J. Vac. Sci. Technol.* B1: 723-25

64. Vanderbilt, D., Louie, S.G. 1984. *Phys. Rev.* B30: 6118-30

65. Badziag, P. 1988. *The Structure of Surfaces II*, Springer Ser. Surf. Sci., 11: 316-19. Berlin: Springer-Verlag

66. Ramaker, D.E., Hutson, F.L. 1987. *Solid State Commun.* 63: 335-39

67. Kubiak, G.D., Kolasinski, K.W. 1989. *Phys. Rev.* B39: 1381-84

68. Hamza, A.V., Kubiak, G.D. 1989. *J. Vac. Sci. Technol.* B7: 1165-70

69. Valone, S.M., Trkula, M., Laia, J.R. 1990. *J. Mater. Res.* 5: 2296-2304

70. Patterson, D.L., Hauge, R.E., Margrave, J.L. 1989. In *New Materials Approaches to Tribiology: Theory and Applications*, Mater. Res. Soc. Symp. Proc. 140: 351-56

71. Hsu, D.S.Y., Turner, N.H. July 1989. *4th SDIO/IST Diamond Technol. Initiative Symp.*, Crystal City, Va. Unpulbished

72. Himpsel, F.J., Knapp, J.A., Van Vechten, J.A., Eastman, D.E. 1979. *Phys. Rev.* B20: 624-27

73. Kvaskov, V.B., Gorbachev, V.V. 1988. *Sov. Phys. Semicond.* 22: 314-15

74. Geis, M.W., Gregory, J.A., Pate, B.B. 1991. *IEEE Trans. Electron. Dev.* 38: 619-26

75. Maguire, H.G. 1976. *Phys. Status Solidi B*76: 715-26

76. Hamza, A.V., Kubiak, G.D., Stulen, R.H. 1990. *Surf. Sci.* 237: 35-52

77. Celii, F.G., Purdes, A.J., Gnade, B.E., Weathers, D.L. 1991. In *New Diamond Science and Technology* (Proc. 2nd Int. Conf. New Diamond Sci. Technol.), ed. R. Messier, J.T. Glass, pp. 631-36. MRS Int. Conf. Proc. Ser. Pittsburgh: Mater. Res. Soc.

78. Freedman, A., Stinespring, C.D. 1990. *Appl. Phys. Lett.* 57: 1194-96

79. Kamo, M., Yurimoto, H., Sato, Y. 1988. *Appl. Surf. Sci.* 33/34: 553-60

80. Geis, M.W. 1990. In *Diamond, Boron Nitride, Silicon Carbide and Related High Bandigap Semiconductors*, Mater. Res. Soc. Symp. Proc., 162: 15-22

81. Chu, C.J., D'Evelyn, M.P., Hauge, R.H., Margrave, J.L. 1990. *Carbon* 28: 805

82. Badzian, A., Badzian, T., Wang, X.H. 1990. *Carbon* 28:804

83. Badzian, A., Badzian, T., Wang, X.H., Hartnett, T.M. 1991. See Rel. 77, pp. 549-56

84. Fujimori, N., Imai, T., Nakahata, H., Shiomi, H., Nishibayashi, Y. 1990. See Ref. 80, pp. 23-33

85. Hoffmann, F.M. 1983. *Surf. Sci. Rep.* 3: 107-92

85a. Jansen, F., Machonkin, M.A., Kuhman, D.E. 1990. *J. Vac. Sci. Technol.* A8: 3785-90

86. Bachmann, P.K., Drawl, W., Knight, D., Weimer, R., Messier, R.F. 1988. In *Diamond and Diamond-Like Materials Synthesis*, extended abstracts ed. G.H. Johnson, A.R. Badzian, M.W. Geis, Mater. Res. Soc. EA-15, pp. 99-102

87. Ravi, K.V., Koch, C.A. 1990. *Appl. Phys. Lett.* 57: 348-50

88. Ravi, K.V., Koch, C.A., Hu, H.S., Joshi, A. 1990. *J. Mater. Res.* 5: 2356-66

89. DeNatale, J.F., Flintoff, J.F., Harker, A.B. 1990. *J. Appl. Phys.* 68: 4014-19

90. Celii, F.G., Nelson, H.H., Pehrsson, P.E. 1990. *J. Mater. Res.* 5: 2337-44

91. Iijima, S., Aikawa, Y., Baba, K. 1990. *Appl. Phys. Lett.* 57: 2646-48

92. Bar-Yam, Y., Moustakas, T.D. 1989. *Nature* 342: 786-87

93. Machlin, E.S. 1988. *J. Mater. Res.* 3: 958-68

94. Joffreau, P.O., Haubner, R., Lux, B. 1988. *Int. J. Refract. Hard Metals* 7: 186-94

95. Joffreau, P.O., Bichler, R., Haubner, R., Lux, B. 1988. *Int. J. Refract. Hard Metals* 7: 92-97

96. Lee, Y.H., Bachmann, K.J., Glass, J.T., LeGrice, Y.M., Nemanich, R.J. 1990. *Appl. Phys. Lett.* 57: 1916-18

97. Meilunas, R., Wong, M.S., Sheng, K.C., Chang, R.P.H., Van Duyne, R.P. 1989. *Appl. Phys. Lett.* 54: 2204-6

98. Williams, B.E., Glass, J.T. 1989. *J. Mater. Res.* 4: 373-84

99. Glass, J.T., Williams, B.E., Davis, R.F. 1988. *SPIE Conf. Proc.* 877:56-63

100. Williams, B.E., Glass, J.T., Davis, R.F., Kobashi, K. 1990. *J. Cryst. Growth* 99: 1168-76

101. Collins, R.W., Cong, Y., Kim, Y.-T., Vedam, K., Liou, Y., et al. 1989. *Thin Solid Films* 181: 565-78

102. Kobayashi, K., Karasawa, S., Watanabe, T., Togashi, F. 1990. *J. Cryst. Growth* 99: 1211-14

103. Badzian, A.R., Badzian, T., Roy, R., Messier, R., Spear, K.E. 1988.*Mater. Res. Bull.* 23: 531-48

104. Belton, D.N., Harris, S.J., Schmieg, S.J., Weiner, A.M. 1989. *Appl. Phys. Lett.* 54: 416-17

105. Belton, D.N., Schmieg, S.J. 1989. *J. Appl. Phys.* 66: 4223-29

106. Harris, S.J., Belton, D.N., Weiner, A.M., Schmieg, S.J. 1989. *J. Appl. Phys.* 66: 5353-59

107. Belton, D.N., Schmieg, S.J. 1990. *Surf. Sci.* 233: 133-40

108. Belton, D.N., Schmieg, S.J. 1990. *J. Vac. Sci. Technol.* A8: 2353-62

109. Turner, K.F., LeGrice, Y.M., Stoner, B.R., Glass, J.T., Nemanich, R.J. 1991. *J. Vac. Sci. Technol.* B9: 914-19

110. Hartnett, T., Miller, R., Montanari, D., Willingham, C., Tustison, R. 1990. *J. Vac, Sci. Technol.* A8: 2129-36

111. Yoshikawa, M., Ishida, H., Ishitani, A., Murakami, T., Koizumi, S., Inuzuka, T. 1990. *Appl. Phys. Lett.* 57: 428-30

112. Koizumi, S., Murakami, T., Inuzuka, T., Suzuki, K. 1990. *Appl. Phys. Lett.* 57: 563-65

113. Morrish, A.A., Pehrsson, P.E. 1991. *Appl. Phys. Lett.* 59: 417-419

114. Frenklach, M., Kematick, R., Huang, D., Howard, W., Spear, K.E., et al. 1989. *J. Appl. Phys.* 66: 395-99

115. Prins, J.F., Gaigher, H.L. 1991. See Ref. 77, pp. 561-66

116. Robertson, J.L., Moss, S.C., Lifshitz, Y., Kasi, S.R., Rabalais, J.W., et al. 1989. *Science* 243: 1057-50

117. Moss, S.C. 1989, *Science* 244: 1029-30

118. Kurihara, K., Sasaki, K., Kawarada, M., Koshino, N. 1988. *Appl. Phys. Lett.* 52: 437-38

119. Tzeng, Y., Cutshaw, C., Philips, R., Srivinyunon, T., Ibrahim, A., Loo, B.H. 1990. *Appl. Phys. Lett.* 56: 134-36

120. Bar-Yam, Y., Moustakas, T.D. 1990. See Ref. 80, pp. 201-4

121. Matsumoto, S., Matsui, Y. 1983. *J. Mater. Sci.* 18: 1785-95

122. Kobashi, K., Nishimura, K., Kawate, Y., Horiuchi, T. 1988. *Phys. Rev.* B38: 4067-84

123. Kim, J.S., Kim, M.H., Park, S.S., Lee, J.Y. 1990. *J. Appl. Phys.* 67: 3354-57

124. Kobashi, K., Nishimura, K., Kawate, Y. Horiuchi, T. 1988. *J. Vac. Sci. Technol.* A6: 1816-17

125. Badzian, A.R. 1988. In *Advance in X-ray Analysis*, ed. C.S. Barrett, J. B. Gilfrich, R. Jenkins, J.C. Russ, J.W. Richarson, P.K. Predecki, 31: 113-28. New York: Plenum

126. Clausing, R.E., Heatherly L., More, K.L., Begun, G.M. 1989. *Surf. Coatings Technol.* 39/40: 199-210

127. Specht, E.D., Clausing R.E., Heatherly L. 1990. *J. Mater. Res.* 5: 2351-55

128. Kaae, J.L., Gantzel, P.K., Chin, J., West, W.P. 1990. *J. Mater. Res.* 5: 1480-89

129. Celii, F.G., White, D. Jr., Purdes, A. J. 1991. *J. Appl. Phys.* 70:5636

130. Frenklach, M., Spear, K.E. 1988. *J. Mater. Res.* 3: 133-40

131. Huang, D., Frenklach, M., Maroncelli, M. 1988. *J. Phys. Chem.* 92: 6379-81

132. Kobashi, K., Nishimura, K., Miyata, K., Kumagai, K., Kawate, Y. 1989. *Diamond and Diamond-like Films*, Electrochem. Soc. Proc., 89-12, pp. 296-305. Pennington, NJ

133. Kobashi, K., Nishimura, K., Miyata, K., Kumagai, K., Nakaue, A. 1990. *J. Mater. Res.* 5: 2469-82

134. Narayan, J., Srivatsa, A.R., Peters, M., Yokota, S., Ravi, K.V. 1988. *Appl. Phys. Lett.* 53: 1823-25

135. Geis, M.W. 1989. *Appl. Phys. Lett.* 55: 550-52

136. Jeng, D.G., Tuan, H.S., Salat, R.F., Fricano, G.J. 1990. *Appl. Phys. Lett.* 56: 1968-70

137. Deleted in Proof

138. Wild, Ch., Herres, H., Wagner, J., Koidl, P., Anthony, T.R. 1989. See Ref. 132, pp. 283-95

139. Wild, Ch., Herres, H., Koidl, P. 1990. *J. Appl. Phys.* 68: 973-78

140. Celii, F.G., Pehrsson, P.R., Wang, H.-t., Butler, J.E. 1988. *Appl. Phys. Lett.* 52: 2043-45

141. Celii, F.G., Pehrsson, P.E., Wang, H.-t., Nelson, H.H., Butler, J.E. 1990. *Proc. 1st Int. Conf. New Diamond Sci,*

Technol. October 1988, ed. S. Saito, M. Yoshikawa, pp.17-23. Tokyo: KTK Scientific, Terra Scientific

142. Celii, F.G., Butler, J.E. 1989. See Ref. 132, pp. 317-29
143. Harris, S.J., Weiner, A.M., Perry, T.A. 1988. *Appl. Phys. Lett.* 53: 1605-6
144. Harris, S.J., Weiner, A.M. 1990. *J. Appl. Phys.* 67: 6520-26
145. Wu, C.-H., Tamor, M.A., Potter, T.J., Kasier, E.W. 1990. See Ref. 80, pp. 133-38
146. Wu, C.-H., Tamor, M.A., Potter, T.J., Kasier, E.W. 1990. *J. Appl. Phys.* 68: 4825-29
147. Chu, C.J., D'Evelyn, M.P., Hauge, R.H., Margrave, J.L. 1990. See Ref. 80, pp. 85-90
148. Chu C.J., D'Evelyn, M.P., Huage, R.H., Margrave, J.L. 1990. *J. Mater. Res.* 5: 2405-13
149. Celii, F.G., Pehrsson, P.E., Wang, H,-t., Nelson, H.H., Butler, J.E. 1989. *Advances in Laser Science IV*, ed. J.L. Gole, D.F. Heller, M. Lapp, W.C. Stwalley, No. 191, pp. 747-49. AIP Conf. Proc.
150. Celii, F.G., Butler, J.E. 1989. *Appl. Phys. Lett.* 54: 1031-33
151. Celii, F.G., Pehrsson, P.E., Butler, J.E. 1989. *Proc. SPIE Conf. Diamond Opt. II* 1146: 119-23
152. Celii, F.G., Butler, J.E. 1991. See Ref. 77, pp. 201-6
153. Sommer, M., Smith, F.W. 1990. See Ref. 80, pp. 139-44
154. Chang, C.-P., Flamm, D.L., Ibbotson, D.E., Mucha, J.A. 1988. *J. Appl. Phys.* 63: 1744-48
155. Hirose, Y., Terasawa, Y. 1986. *Jpn. J. Appl. Phys.* 25: L519-21
156. Saito, Y., Sato, K., Gomi, K., Miyadera, H. 1990. *J. Mater. Res.* 25: 1246-50
157. Kawato, T., Kondo, K. 1987. *Jpn. J. Appl. Phys.* 26: 1429-32
158. Harris, S.J., Weiner, A.M. 1989. *Appl. Phys. Lett.* 55: 2179-81
159. Sommer, M., Smith, F.W. 1991. *J. Vac. Sci. Technol.* A9: 1134-39
160. Meier, U., Kohse-Hoinghaus, K., Schafer, L., Klages, C.-P. 1990. *Appl. Opt.* 29: 4993-99
161. Schafer, L., Klages, C.-P., Meier, U., Kohse-Hoinghaus, K. 1991. *Appl. Phys. Lett.* 58: 571-73
162. Jansen, F., Chen, I., Machonkin, M.A. 1989. *J. Appl. Phys.* 66: 5749-55
163. Roman, W.C., Colket, M.B. III, Hay, S.O., Eckbreth, A.C. 1989. See Ref. 132, pp. 330-41
164. Hay, S.O., Roman, W.C., Colket, M.B. III. 1990. *J. Mater. Res.* 5:2387-97
165. Matsumoto, O., Toshima, H., Kanzaki, Y. 1985. *Thin Solid Films* 128: 341-51
166. Saito, Y., Matsuda, S., Nogita, S. 1986. *J. Mater. Sci. Lett.* 5: 565-68
167. Mitsuda, Y., Kojima, Y., Yoshida, T., Akashi, K. 1987. *J. Mater. Sci.* 22: 1557-62
168. Saito, Y., Sato, K., Tanaka, H., Fujita, K., Matuda, S. 1987. *J. Mater. Sci.* 23: 842-46
169. Flamm, D.L., Herb, G.K. 1989. In *Plasma Etching*, ed. D.M. Manos, D.L. Flamm, pp. 1-89. New York: Academic
170. Coburn, J.W., Chen, M. 1980. *J. Appl. Phys.* 51: 3134-36
171. Mucha, J.A., Flamm, D.L., Ibbotson, D.E. 1989. *J. Appl. Phys.* 65: 3448-52
172. Inspektor, A., McKenna, T., Liou, Y., Bourget, L., Spear, K.E., Messier, R. 1989. See Ref. 132, pp.342-52
173. Inspektor, A., Liou, Y., McKenna, T., Messier, R. 1989. *Surf. Coatings Technol.* 39/40: 211-21
174. Zhu, W., Inspektor, A., Badzian, A., McKenna, T., Messier, R. 1990. *J. Appl. Phys.* 68: 1489-96
175. Saito, Y., Sato, K., Gomi, K., Miyadera, H. 1990. *J. Mater. Res.* 25: 1246-50
176. Muranaka, Y., Yamashita, H. Sato, K., Miyadera, H. 1990. *J. Appl. Phys.* 67: 6247-54
177. Hayashi, N., Etoh, Y., Kazahaya, T., Katsumata, S., Aketagawa, M. 1991. See Ref. 77, pp. 473-78
178. Chu, H.N., Lefkow, A.R., Den Hartog, E.A., Jacobs, J., Sandstrom, P., et al. 1990. See Ref. 80, pp. 163-66
179. Chu, H.N., Den Hartog, E.A., Lefkow, A.R., Jacobs, J., Anerson, L.W., et al. 1991. *Phys. Rev.* A44: 3796-3803
180. Celii, F.G., Thorsheim, H.R., Butler, J.E., Plano, L.S., Pinneo, J.M. 1990. *J. Appl. Phys.* 68: 3814-17
181. Thorsheim, H.R., Celii, F.G., Butler, J.E., Plano, L.S., Pinneo, J.M. 1991. See Ref. 77, pp. 207-12
182. Hsu, W.L., Tung, D.M. 1991. See Ref. 77, pp. 239-44
183. Plano, L.S., Stevenson, D.A., Carruthers, J.R. 1991. See Ref. 77, pp. 257-62
184. Toyoda, H., Kojima, H., Sugai, H. 1989. *Appl. Phys. Lett.* 54: 1507-9
185. Fujimori, N., Ikegaya, A., Imai, T., Fukushima, K., Ota, N. 1989. See Ref. 132, pp. 465-74
186. Koshino, N., Kurihara, K., Kawarada, M., Sasaki, K. 1988. See Ref. 86, pp. 95-98
187. Suzuki, K., Sawabe, A., Inuzuka, T. 1988. *Appl. Phys. Lett.* 53: 1818-20
188. Suzuki, K., Sawabe, A., Inuzuka, T. 1990. *Jpn. J. Appl. Phys.* 29: 153-57
189. Zhang, F., Zhang, Y., Yang, Y., Chen, G., Jiang, X. 1990. *Appl. Phys. Lett.* 57: 1467-69
190. Raiche, G.A., Smith, G.P., Jeffries, J.B. 1991. See Ref. 77, pp. 251-56

191. Mitsuda, Y., Tanaka, K., Yoshida, T. 1990. *J. Appl. Phys.* 67: 3604-8

192. Hirose, Y., Amanuma, S., Okada, N., Komaki, K. 1989. See Ref. 132, pp. 80-92

193. Matsui, Y., Yuuki, A., Sahara, M., Hirose, Y. 1989. *Jpn. J. Appl. Phys.* 28: 1718-24

194. Matsui, Y., Yake, H., Hirose, Y. 1990. *Jpn. J. Appl. Phys.* 29: 1552-60

195. Cappelli, M.A., Paul, P.H. 1990. *J. Appl. Phys.* 67: 2596-2602

196. Ye, C., Suto, M., Lee, L.C. 1988. *J. Cehm. Phys.* 89: 2797-2802

197. Morrison, P. Jr., Cosgrove, J.E., Markham, J.R., Solomon, P.R. 1990. *Carbon* 28: 767-69

198. Morrison, P. Jr., Cosgrove, J.E., Markham, J.R., Solomon, P.R. 1991. See Ref. 77, pp. 219-24

199. Chauhan, S.P., Angus, J. C., Gardner, N.C. 1976. *J. Appl. Phys.* 47: 4746-54

200. Anthony, T.R. 1990. See Ref. 80, pp. 61-74

200a. Anthony, T.R. 1990. *Vacuum* 41: 1356-59

201. Vakil, H.B., Banholzer, W.F., Kehl, R.J., Spiro, C.L. 1989. *Mater. Res. Bull.* 14: 733-38

202. Martin, L.R., Hill, M.W. 1989. *Appl. Phys. Lett.* 55: 2248-49

203. Martin, L.R., Hill, M.W. 1990. *J. Mater. Sci. Lett.* 9: 621-23

204. Patterson,D.E., Bai, B.J., Chu, C.J., Hauge, R.H., Margrave, J.L. 1991. See Ref. 77, pp. 433-38

205. Rudder, R.A., Posthill, J.B., Markunas, R.J. 1989. *Electron. Lett.* 25: 1220-21

206. Piekarczyk, W., Roy, R.W., Yarbrough, W.A. 1989. *J. Cryst. Growth* 98: 765-76

207. Piekarczyk, W., Yarbrough, W.A. 1991. *J. Cryst. Growth* 108: 583-97

208. Sommer, M., Mui, K., Smith, F.W. 1989. *Solid State Commun.* 69: 775-78

209. Sommer, M., Smith, F.W. 1990. *J. Mater. Res.* 5: 2433-40

210. Kosky, P.G., McAtee, D.S. 1989. *Mater. Lett.* 8: 369-74

211. Frenklach, M. 1989. *J. Appl. Phys.* 65: 5142-49

212. Frenklach, M., Wang, H. 1991. *Phys. Rev.* B43: 1520-45

213. Chem, I. 1988. *J. Appl. Phys.* 64: 3742-45

214. Matsui, Y., Sahara, M. 1989. *Jpn. J. Appl. Phys.* 28: 1023-29

215. Harris, S.J. 1989. *J. Appl. Phys.* 65: 3044-48

216. Harris, S.J., Martin, L.R. 1990. *J. Mater. Res.* 5: 2313-19

217. Goodwin, D.G., Gavillet, G.G. 1990. *J. Appl. Phys.* 68: 6393-6400

218. Goodwin, D.G., Gavillet, G.G. 1991. See Ref. 77, pp. 335-40

219. Tsuda, M., Nakajima, M., Oikawa, S. 1986. *J. Am. Chem. Soc.* 108: 5780-83

220. Tsuda, M., Nakajima, M., Oikawa, S. 1987. *Jpn. J. Appl. Phys.* 26: L527-29

221. Harris, S.J. 1990. *Appl. Phys. Lett.* 56: 2298-2300

222. Benson, S.W. 1976. *Thermochemical Kinetics.* New York: Wiley

223. Page, M., Brenner, D.W. 1990. See Ref. 77, pp. 45-50

224. Goodwin, D.G. 1991. *Appl. Phys. Lett.* 59: 277-279

225. Mintmire, J.W., Brenner, D.W., Dunlap, B.I., Mowrey, R.C., White, C.T. 1991. See Ref. 66, pp. 57-62

226. Pederson, M.R., Jackson, K.A., Pickett, W.E. 1990. See Ref. 80, pp. 91-98

227. Pederson, M.R., Jackson, K.A., Pickett, W.E. 1989. In Technology Update on Diamond Films, extended abstracts, ed. R.P.H. Chang, D. Nelson, A. Hiraki, Mater. Res. Soc. EA-19, pp. 157-61

228. Brenner, D.W., Dunlap, B.I., Mintmire, J.W., Mowrey, R.C., White C. T. 1991. See Ref. 77, pp.39-44

SCANNING ELECTRON MICROGRAPHS OF DIAMOND STALAGMITES GROWN IN AN OXYGEN-ACETYLENE TORCH (Photo credit - Henry Hoff, NRL)

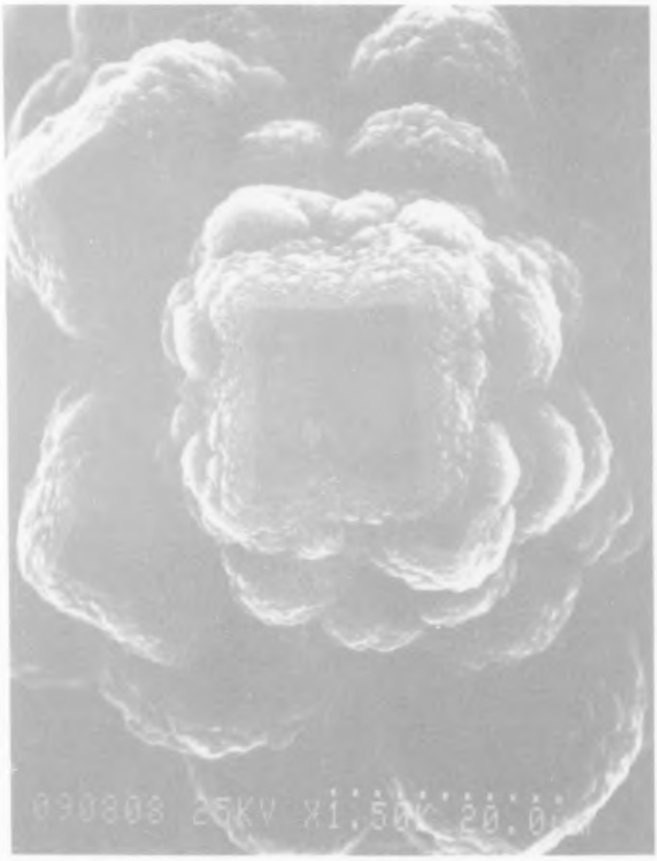

DEPARTMENT OF THE NAVY
OFFICE OF NAVAL RESEARCH
ARLINGTON, VA 22217

OFFICIAL BUSINESS
PENALTY FOR PRIVATE USE, $300